

NASA Contractor Report 201687



# Spin-Tunnel Investigation of a 1/28-Scale Model of the NASA F-18 High Alpha Research Vehicle (HARV) With and Without Vertical Tails

C. Michael Fremaux

*Lockheed Martin Engineering & Sciences Company, Hampton, Virginia*

Contract NAS1-19000

April 1997

National Aeronautics and  
Space Administration  
Langley Research Center  
Hampton, Virginia 23681-0001

## Abstract

An investigation was conducted in the NASA Langley 20-Foot Vertical Spin Tunnel to determine the developed spin and spin-recovery characteristics of a 1/28-scale, free-spinning model of the NASA F-18 HARV (High Alpha Research Vehicle) airplane that can be configured with and without the vertical tails installed. The purpose of the test was to determine what effects, if any, the absence of vertical tails (and rudders) had on the spin and spin-recovery capabilities of the HARV. The model was ballasted to dynamically represent the full-scale airplane at an altitude of 25 000 feet. Erect and inverted spin tests with symmetric mass loadings were conducted with the free-spinning model. The model results indicate that the basic airplane with vertical tails installed (with unaugmented control system) will exhibit fast, flat erect and inverted spins from which acceptable recoveries can be made. Removing the vertical tails had little effect on the erect spin mode, but did degrade recoveries from erect spins. In contrast, inverted spins without the vertical tails were significantly more severe than those with the tails installed.

## Introduction

Currently, there is an interest in exploring the feasibility of flight without the use of vertical stabilizers. The maturation of thrust vectoring has allowed designers to begin considering tailless designs as a means of reducing drag, for example. But the primary driver behind this interest is the pursuit of low radar cross section (RCS), or "stealth" characteristics that are superior to those available on contemporary designs such as the F-117A and F-22. On these configurations, radar-reflecting vertical tails must be compensated for using various stealth techniques. However, it is unlikely that any current technology could be expected to provide the low-RCS characteristics that could be realized by removing a source of radar reflections altogether.

An investigation was conducted in the NASA Langley 20-Foot Vertical Spin Tunnel to determine what effects, if any, the lack of vertical

tails had on the spin and spin-recovery characteristics of a 1/28-scale free-spinning model of the NASA F-18 HARV airplane. The HARV was chosen as the subject for this study because it represents a current fighter configuration and is equipped with thrust vectoring which could be used to compensate for the lack of vertical tails. This investigation consisted of developed (i.e., equilibrium) erect and inverted spins and recoveries, with and without the vertical tails installed. Both erect and inverted tests were conducted. Data, in the form of motion time histories, were obtained via an optical data acquisition system installed in the Spin Tunnel (ref. 1).

Note that the present test was not an exhaustive free spin test (e.g., the F/A-18 test described in reference 2). In a typical free spin test program, a model is launched into the Spin Tunnel upwards of one thousand times. With such a large number of tests, all of the equilibrium spin modes that will be possible for the airplane in question are identified. In contrast, the current test program was meant only to identify major trends in the results that resulted from varying geometric parameters on a model whose basic spin modes were already well documented. Therefore, all of the spin modes possible with the modified model may not have been identified in the present test.

## Symbols

$b$	wing span, ft
$\bar{c}$	wing mean aerodynamic chord, ft
$C_n$	body axis yawing moment coefficient
$I_x, I_y, I_z$	moment of inertia about the x, y, or z body axis, respectively, slug-ft <sup>2</sup>
$\ell$	linear dimension, ft
$m$	mass of model or airplane, slugs
$N$	model-to-airplane scale ratio
$S$	wing area, ft <sup>2</sup>
$Re$	Reynolds number, $\frac{V\ell}{\nu}$

V	full-scale rate of descent, ft/s	IPMP	inertia pitching moment parameter, $\frac{I_z - I_x}{mb^2}$
$\alpha$	calculated angle of attack at model or airplane center of rotation, $\alpha = \arctan(\tan(\bar{\alpha})\cos(\phi))$ , deg	IRMP	inertia rolling moment parameter, $\frac{I_y - I_z}{mb^2}$
$\bar{\alpha}$	$\theta + 9$ , angle between model fuselage reference waterline and vertical in Spin Tunnel, deg	IYMP	inertia yawing moment parameter, $\frac{I_x - I_y}{mb^2}$
$\beta$	calculated sideslip angle at model or airplane center of rotation, $\beta = \arcsin(\sin(\bar{\alpha})\sin(\phi))$ , deg	MSPS	Model Space Positioning System, Spin Tunnel data acquisition system
$\delta_a$	aileron deflection, deg	RCS	radar cross section
$\delta_d$	differential horizontal stabilizer deflection, deg	U	inner wing up, or control surface deflected trailing edge up
$\delta_f$	leading-edge flap deflection, deg	W	with the spin
$\delta_r$	rudder deflection, deg	<b>Model</b>	
$\phi$	roll angle, deg		
$\mu$	relative density of model or airplane, $m/\rho S b$		
$\nu$	kinematic viscosity of air, $ft^2/s$		
$\rho$	density of air, $slugs/ft^3$		
$\sigma$	ratio of air density at altitude to that at sea level		
$\theta$	pitch angle, deg		
$\Omega$	full-scale spin rate about vertical axis, deg/s		
$\psi$	yaw angle, deg		

Abbreviations:

A	against the spin
c. g.	center of gravity
D	leading-edge flap deflected down, or other control surface deflected trailing-edge down
DOF	degrees of freedom

An existing 1/28-scale model of the NASA F-18 High Alpha Research Vehicle (HARV), fabricated at the NASA Langley Research Center, was tested in the Langley 20-Foot Vertical Spin Tunnel. The thrust vectoring vanes and actuators on the HARV airplane were not represented on the model. The model was modified so that the vertical tails were removable at the surface of the fuselage. The rudders could be actuated for tests with the tails installed. The dimensional characteristics of the airplane are presented in table 1. A three-view drawing of the unmodified model appears in figure 1. A drawing of the model with the vertical tails removed appears in figure 2. Photographs of the model as-tested with the vertical tails installed appear in figure 3.

The model was ballasted to obtain dynamic similarity to the airplane at an altitude of 25 000 ft ( $\rho = 1.065 \times 10^{-3}$  slug/ft<sup>3</sup>) using Froude scaling. The dynamic scaling relationships, discussed in detail in references 3 and 4, are presented in table 2. The mass characteristics, center of gravity, and moment of inertia parameters used for the airplane and for the model as-tested are presented in table 3.

Remotely controlled servo-actuators installed in the model for moving the controls provided sufficient torque on the controls to reverse them fully and rapidly for the recovery attempts. The normal maximum control surface deflections of the airplane were not all fully utilized used on the model. For this investigation, the control deflections used (with respect to the surface's trailing edge and measured perpendicular to the hinge lines) were as follows:

Pitch control:

Horizontal stabilizer  
(average deflection), deg .....14 up, 0 down

Roll control:

Ailerons, deg.....25 up, 25 down  
Differential horizontal  
stabilizer, deg.....± 20 from average  
deflection  
(i.e., 10 up, 10 down)

Yaw control:

Rudders  
(when installed), deg.....30 right, 30 left

The deflections of each control surface used during the tests are those shown in tables 4 and 5. The time history plots in figures 4 through 9 also indicate the rudder deflections used during the tests, where applicable.

### Spin Tunnel Tests

The free-spin tests of the model were performed in the Langley 20-Foot Vertical Spin Tunnel, which is described in reference 5. The techniques used in free-spin testing are also described in detail in reference 5 and a brief summary is given in the appendix of this report. A discussion of the methods and procedures of spin-tunnel testing, including limitations of the facilities and an indication of the interpretation of the quantitative model results to predict full-scale characteristics, is also included in the appendix.

A recently developed data acquisition system was used to obtain 6-DOF motion time histories of the F-18 HARV model during equilibrium spins and recoveries. The Spin Tunnel Model Space Positioning System (MSPS) is a non-intrusive, workstation-based system that uses a single camera view to generate post-test estimates of model attitude and position at a sample rate of 60 Hz. Numerical differentiation is used to calculate angular rates. Further discussion of this system can be found in reference 1. Data in the time-history plots as well as the summary tables (with the exception of number of turns for recovery and the sink rate, V) were generated using the MSPS.

### Reynolds Number Effects

Spin tunnel tests are conducted at Reynolds numbers on the order of  $1.0 \times 10^5$ , which are significantly lower than those obtained for full-scale airplanes at flight conditions. Changes in aerodynamic characteristics due to Reynolds number effects have been found to have a substantial impact on the spin characteristics of some configurations (ref. 5). For modern high-performance fighter designs having wings with sharp leading edges, the most common source of Reynolds number effects at spinning conditions is a change in the forebody crossflow. In the absence of high Reynolds number data obtained on a rotary balance, high Reynolds number static data at high angles of attack and large sideslip angles are typically used to determine whether or not a configuration will be sensitive to Reynolds number effects at spinning attitudes. These data were not available specifically for the F-18 HARV. However, unpublished results of high Reynolds number static tests noted in reference 2 indicate that the F/A-18A is not sensitive to these effects. Since the forebodies of the F/A-18A and the F-18 HARV (which is a modified F/A-18C) are similar, it was assumed that Reynolds number effects could be neglected for the present tests.

### Results and Discussion

The results of the model spin tests (with explanatory notes) are presented in tables 4 and 5, and figures 4 through 11 with model data given in

terms of full-scale values for the airplane at an altitude of 25 000 feet. Erect spin results are discussed first, followed by results for inverted spins. Results for each control combination tested are identified by a test number in tables 4 and 5. Erect and inverted tests with the tails installed were made with the rudders actuated and also with the rudders maintained at neutral during both the spin and the recovery. The number of turns for recovery (obtained from the video-tape records of each test) are noted in tables 4 and 5. Spins to the pilot's left were used exclusively in this series of tests, based on earlier tests with the HARV model in which it was determined that the left spin was the critical (i.e., the faster spin rate) erect case. Inverted spins were also done to the pilot's left for consistency. However, the results should generally apply to spins in either direction.



The spin block symbol  used in tables 4 and 5, and figures 4 through 9, provides a simplified, quick reference for indicating the lateral and longitudinal control-surface positions of the model (with respect to a ground-based observer) for each test. For the airplane, these control-surface positions are the result of commands from the pilot and the flight control system. In spin-tunnel tests, the flight control laws are not directly modeled, so each spin block shows control surface positions that would be commanded for an assumed flight condition. For descriptions made in terms of pilot command (e.g., stick forward), the meaning applies to a conventional, unaugmented control system (i.e., a direct link between the control stick and the control surfaces). On the spin block, the top horizontal line represents the horizontal stabilizers fully trailing-edge up (stick back for erect spins, stick forward for inverted spins), the middle horizontal line represents stabilizers neutral, and the bottom horizontal line indicates stabilizers fully trailing-edge down (stick forward for erect spins, stick back for inverted spins). The left vertical line represents roll controls (i.e., ailerons and differential horizontal tails) fully against the spin (stick right in an erect spin to the pilot's left, stick left in an inverted spin to the pilot's left), the middle vertical line represents roll controls neutral, and the right vertical line represents roll controls with, or into, the spin (stick left in an erect spin to the pilot's left, stick right in an inverted spin to the pilot's left). Footnotes to the tables and

specific control deflection information are provided to clarify each spin block. The dot represents the control positions for the developed spin, and the arrow indicates the movement of these controls for the recovery attempt.

### Erect Spin and Spin-Recovery Tests

Summaries of the results for the erect spin and spin-recovery tests are found in table 4. Time history plots of the erect tests (angle of attack, sideslip angle, and spin rate) are found in figures 4 through 6. Gaps in the time histories (e.g., fig. 4b) indicate that the MSPS camera lost track of the model for an interval of time before re-acquiring it.

In the three cases summarized in table 4, the erect equilibrium spins obtained were fast and flat with average angles of attack of 85° to 86° and average sideslip angles of 2° to 4°. The measured angles of attack and sideslip angles were somewhat oscillatory, as indicated by the maximum and minimum values given in the table and clearly shown in the corresponding time history plots. The full-scale rates of descent were 285 ft/s for all cases. It is clear from table 4 that there was little change in the equilibrium spins that can be correlated to the removal of the vertical tails, as would be expected for an erect, flat spin in which these surfaces were immersed in the low-energy wake produced by the wing, stabilizers, and fuselage. Likewise, comparing the results of test 1 (rudders neutral) and test 2 (rudders prospin) illustrates that the deflection of the rudders with the tails installed had little effect on the characteristics of the developed flat spin mode other than to produce a slightly faster average spin rate for the prospin-rudders case.

In contrast, spin recoveries were impacted by the removal of the vertical tails (and rudders). With the rudders maintained at neutral (test 1 - table 4), recoveries with the tails installed required up to 2 1/2 turns, while for the tails removed (test 3) the recoveries were slightly longer at 2 3/4 to 3 turns. Obviously, as the angle of attack decreased during the recoveries, the vertical tails became less "blanked" by the low energy wake, presumably making the tails-on configuration more damped in yaw during recovery

than the tails-removed case. The negative impact on the recoveries caused by reducing vertical tail size is more pronounced when comparing the tails-off results to the tails-on results with the rudders actuated. With the rudders deflected fully against the spin for the recoveries (test 2), the number of turns for recovery was reduced by half as compared to the maximum number of turns required in the tails-off case (1 1/2 turns versus 3 turns, respectively).

The relative impact on recovery from erect spins caused by removing the vertical tails is also illustrated in figure 10, in which only the recovery segments of the spin rate ( $|\Omega|$ ) time histories of figure 6a (vertical tails installed - rudders neutral), figure 6b (tails installed - rudders against the spin for recovery), and figure 6c (tails removed) are re-plotted. In figure 10, the origin of the time axis (abscissa) has been shifted from those in figure 6 and corresponds to the initial input of recovery controls (roll controls with the spin in all three cases plus rudders against the spin for the rudders-actuated case). Note that the length of scaled time for which data were obtained (here between 6 and 7 seconds) represents the time that MSPS was able to track the model, and not necessarily the time required for full recoveries (i.e.,  $|\Omega| = 0$ ) to be realized. The number of turns for recovery summarized in tables 4 and 5 were obtained directly from video tape records of the tests.

The spins noted in figure 10 had similar characteristics up to the point of recovery-control input, as noted earlier (tests 1, 2, and 3 - table 4). At approximately 1.5 seconds after recovery control input (time = 0), the curves become nearly linear (except for the final 1.5 seconds from figure 6a), albeit with different slopes. Straight lines were fit through the remaining linear portions of the curves so that the nominal slopes (i.e., the average angular decelerations) could be compared. As shown in figure 10, the spin-rate deceleration of the tails on-rudders neutral case was greater than that for the tails-off case throughout the tracked portions on the recoveries. However, the tails-on/rudders-against results showed significantly greater deceleration during recovery than either of the previous cases. Presumably, this indicates that most of the antispin yawing moment increment

produced during recovery by the vertical tails resulted from the rudders being deflected against the spin.

To verify this assumption, further analysis of these three recoveries was performed. Values of the unsteady aerodynamic yawing moment coefficient produced during recovery were calculated based on the motion time histories in figures 4, 5, and 6. The technique used for the moment calculations is described in reference 6. Briefly, the total external (aerodynamic) moments acting upon the rigid, free-spinning model were calculated using the equations of motion and data from the free spin tests (attitude time histories, mass and inertia characteristics, and test conditions). The sink rate (and thus the dynamic pressure) was assumed to be constant during recovery for the purpose of the calculations.

The calculated values of  $C_n$  are shown in figure 11 where, again, only the recovery portions of the tests have been plotted and recovery control deflection has been set to time=0. This figure is separated into two plots for clarity. In figure 11a, the tails installed-rudders neutral results (test 1) are compared to tails-removed data (test 3), while in figure 11b, results for tails installed-rudders against the spin (test 2) are compared to the tails-removed data. An indication of rudder effectiveness at the conditions of the test is evident in these two plots. Figure 11a shows that the antispin yawing moment produced with the vertical tails installed is only marginally greater than with the tails removed during the portion of the recovery for which data were available. In contrast, it is clear in figure 11b that significantly greater antispin yawing moment was generated with the full size rudders deflected against the spin as compared to either the tails installed-rudders neutral or the tails-removed cases. 2. For reference, values of  $C_n$  from unpublished rotary balance tests of an F-18A model (with vertical tails) are shown in figure 11. These data points were measured under steady rotation at an attitude that is reasonably representative (without using interpolation) of the average free spin values obtained during the first few seconds after recovery control input ( $\alpha=85^\circ$ ,  $\beta=0^\circ$ , and the non-dimensional spin rate,  $|\Omega b/2V|=0.2$ ; see figures 4a, 4b, 5a, 5b, 6a, and 6b).

## Inverted Spin and Spin-Recovery Tests

Inverted spin results of the F-18 HARV with and without the vertical tails installed are presented in figures 7 through 9. Summaries of these tests are contained in table 5.

In contrast to the erect spins, the results from this series of tests indicate a clear correlation between the inverted spin characteristics of the HARV and whether or not the vertical tails were installed. With the tails installed and the rudders maintained neutral (test 4 - table 5 and figures 7a, 8a, and 9a), it was not possible to maintain an equilibrium spin. The model motions became so oscillatory several turns beyond launch that a stable spin could not be maintained. In contrast, when the model was tested with the rudders deflected with the spin a stable, though highly oscillatory inverted spin was obtained (test 5 - table 5 and figures 7b, 8b, and 9b).

A flatter, significantly less oscillatory inverted spin resulted when the vertical tails were removed. As shown in test 6 of table 5 and figures 7c, 8c, and 9c, the average angle of attack increased (i.e., became more negative) by 5 degrees and the amplitude of the sideslip angle oscillations decreased substantially as compared to the results of test 5 (tails installed - rudders with the spin). Recalling the previous discussion on the relatively minor effects that the vertical tails had on the erect spin and noting the near-symmetry between the upper- and lower halves of the model with the vertical tails removed, it is not surprising that the inverted spin characteristics of the HARV without vertical tails more strongly resembled the erect spin mode (with or without vertical tails) than did the inverted spins with the tails installed.

The effect of the vertical tails during spin recovery is less obvious in the inverted case than in the erect case. All other things being equal, better recoveries are generally obtained from a slower spin than from a faster spin. Likewise, an oscillatory spin will typically result in shorter recoveries than a relatively smooth spin. The vertical tails were shown to have little effect on the erect spin (all were fast and relatively smooth), so that the recoveries noted in table 4 were all essentially starting at the same "initial

conditions" at the time of recovery-control input. Therefore, when differences were noted in the number of turns required for recovery, it was reasonable to assume that the cause was due to some change in the geometric configuration of the model, i.e., whether or not the vertical tails were installed or the rudders were deflected (recall that the mass characteristics were maintained constant tails-installed and tails-removed). Conversely for the inverted tests, the spins were significantly affected by the presence of the vertical tails and by the deflection of the rudders, so that isolating the effect of the tails strictly during the recovery phase of a given test was not possible. In other words, the differences in the inverted-spin recoveries noted in table 5 were caused both by having different initial conditions at recovery-control input and by the (assumed) additional effect of the tails during recovery phase.

Table 5 shows that good recoveries were obtained from spins with the vertical tails installed by neutralizing all controls (2 turns - test 5). As noted above, the spin in test 5 was quite oscillatory, especially in sideslip. When the tails were removed (test 6), resulting in a spin that was faster, flatter, and smoother than the tails-installed case, neutralizing the controls produced severely degraded recoveries of up to 4 1/2 turns. In an attempt to improve recoveries with the vertical tails removed, a final test (test 7) was performed in which the lateral controls were moved to fully with the spin (stick right in an inverted spin to the pilot's left) while maintaining neutral longitudinal control. Good recoveries of 1 1/2 to 1 3/4 turns were realized using this method.

## Conclusions

Based on the results of spin-tunnel tests of a 1/28-scale free-spinning model of the F-18 HARV airplane equipped with removable vertical tails and on other available information on the spinning characteristics of high-performance airplanes, the following conclusions regarding the spin and spin-recovery characteristics of a similarly configured airplane at an altitude of 25 000 feet are drawn:

1. The basic, symmetrically-loaded F-18 HARV airplane with prospin controls (controls crossed, or lateral controls against the spin and rudders

with the spin) will have a fast, flat, relatively smooth erect spin mode. Erect spins obtained with prospin lateral control deflections but with the rudders maintained at neutral, or with the vertical tails removed altogether, will be similar to those obtained with prospin rudder deflections, assuming constant mass characteristics.

2. Good recoveries from erect spins will be obtained by deflecting the lateral controls to with the spin and rudders to against the spin. Recoveries will be degraded if the rudders are maintained at neutral during recovery. Recoveries with the vertical tails removed will require up to twice as many turns as recoveries in which the rudders are deflected against the spin.
3. Inverted spins with prospin controls (controls together, or lateral controls against the spin and rudders with the spin) will be very oscillatory at a high average angle of attack. If the rudders are held at neutral, the oscillations (primarily in sideslip angle) will become so severe that an equilibrium spin mode will be impossible to maintain. With the vertical tails removed, spins will be significantly smoother with a faster spin rate than with the tails installed
4. Good recoveries from inverted spins with the vertical tails installed will be obtained by neutralizing all controls. Neutralizing the longitudinal and lateral controls in order to recover from spins with the vertical tail removed will produce unsatisfactory results. Good recoveries will be obtained if the lateral controls are deflected to fully with the spin while maintaining neutral longitudinal controls (e.g., stick right in an inverted spin to the pilot's left).

## Appendix

### Test Methods and Precision

*Model Testing Technique.* Detailed discussions of spin-model testing techniques, methods of interpreting test results, and correlation

between model and airplane results are presented in reference 5. Spin-tunnel tests are usually performed to predict the spin and spin-recovery characteristics that might be encountered by a full-scale airplane at altitude during planned flight testing or through inadvertent loss of control. This prediction is made based upon the results of extensive free-spinning tests of "dynamically-scaled" models in the Spin Tunnel interpreted in light of the correlation obtained between model tests and flight tests for similar configurations. Model test parameters encompass the full range of airplane loading conditions such as weight, center-of-gravity location, and inertia yawing-moment parameter. Configuration variables such as external stores, flaps, speed brakes, refueling probes, and parachute installations may be investigated. Throughout, a full matrix of control deflections, singly or in combination, including neutral and maximum settings of the control surfaces are typically evaluated.

The controls are preset to the desired prospin deflections and the model is hand launched into the vertically rising air stream. A radio signal is used to control digital-proportional servos which move control surfaces abruptly to the predetermined recovery position. Recovery is typically attempted by movement of the rudder or rudders (if present) and roll controls from prospin to antispin. Control neutralization and rudder reversal alone may also be assessed. Use of pitch control movement for recovery can also be incorporated as required. The critical prospin and optimum recovery control deflections are determined by both the aerodynamic and mass distribution characteristics of the model.

Modern fighter airplanes are generally designed with a relatively long fuselage forebody, which has an added aerodynamic influence on the spin, and a vertical stabilizing surface (or surfaces) that is usually shielded from effective airflow at high angles of attack. The mass characteristics are such that the fuselage is heavily loaded relative to the wings and the relative density,  $\mu$ , is considerably higher than that of airplanes discussed in reference 5. The overall effect of these design characteristics is to cause the roll control surfaces (ailerons and/or differential stabilizers) to become the primary recovery controls.

When investigations are made of modifications to a previously tested model, a greatly reduced matrix of test conditions may be employed. Depending upon the nature of the modifications, only selected critical spins, loadings, and recovery procedures need be assessed.

Primary data acquisition is via the Model Space Positioning System (MSPS), a video-based, computerized data acquisition system. This system is described in reference 1. MSPS produces estimates of the model's six degree-of-freedom attitude and position time histories at a sample rate of 60 Hz using a single-camera view of the test that is recorded and stored on an optical disk and then post-processed. Model angular rates are calculated by numerically differentiating the relevant attitude angle time histories. The angle of attack ( $\alpha$ ) and sideslip angle ( $\beta$ ) at the c.g. are calculated using the formulas

$$\alpha = \arctan(\tan(\bar{\alpha})\cos(\phi)) \quad (1)$$

and

$$\beta = \arcsin(\sin(\bar{\alpha})\sin(\phi)) \quad (2)$$

Equations (1) and (2) are valid assuming the model c.g. and the spin axis are coincident, and that the trajectory of the c.g. is vertical, i.e., there is no translation of the model as it spins. The angles summarized in the tables represent the high, average, and low values measured during the equilibrium portion of a spin (i.e. after the rotation imparted at launch and before the control surfaces are deflected for recovery). Tunnel speed, or "sink rate", is obtained using dynamic pressure measurements from pitot-static tubes in the test section. Full-scale values of the mass properties, angular rates, and sink rate are calculated using the dynamic scaling relationships (refs. 3 and 4).

Data are also obtained from the documentation video record of each test. The number of turns for recovery are counted from the time that the control surfaces are moved to their recovery deflections until the time that the spin rotation ceases. Satisfactory recovery characteristics are established by several factors, rather than by a predetermined number of turns. In reference 5, a 2 1/4-turn criterion is mentioned.

This was based on the experience gained for many model test programs up to that time. Subsequently, the design characteristics of fighter airplanes in particular have changed significantly. For a modern fighter airplane exhibiting a fast, flat spin, a 4-turn recovery might be termed satisfactory after consideration of altitude loss per turn, consistency of recovery, complexity of control manipulation, and sensitivity to deviations from optimum procedure. For recovery attempts in which a model strikes the safety net while it is still in a spin, the recovery is recorded as being greater than the number of turns from the time that the controls were moved to the time that the model struck the net, for example, >3. A ">3-turn" recovery, however, does not necessarily indicate an improvement over a ">7-turn" recovery. A recovery in 10 or more turns is often indicated by the symbol " $\infty$ ". When a model loses the rotation applied at launch within a few turns and recovers without control movement, or oscillations in the pitch and/or roll axes build up until the model rolls out of the initial spinning attitude, no equilibrium spin mode exists and the results are recorded as "no spin."

For spins in which a model has a rate of descent in excess of that which can readily be obtained in the tunnel (typically very steep spins), the rate of descent is recorded as being greater than the velocity at the time that the model hit the safety net, for example, >400 fps full-scale. In such tests, the recoveries are attempted before the model reaches its final steeper attitude and while it is still descending in the tunnel. Such results are considered conservative; that is, recoveries are generally not as fast as when the model is in the final steeper attitude.

If emergency spin-recovery parachute tests are performed, the parachute system required to effect satisfactory recovery is determined. The parachute is deployed for the recovery attempts by actuating a remote-control mechanism, and, unless otherwise noted, the controls are maintained prospin so that recovery is due to the parachute action alone. The number of turns required for recovery are measured from the time the parachute canopy becomes fully inflated until the spin rotation ceases.

**Accuracy.** Data obtained in free-spinning tunnel tests are estimated to be correct values within the following limits:

$\bar{\alpha}$ or $\alpha$ , deg.....	$\pm 1$
$\phi$ or $\beta$ deg.....	$\pm 1$
V, percent .....	$\pm 5$
$\Omega_{avg}$ , percent .....	$\pm 1$
Turns for recovery obtained from video-tape test records .....	$\pm 1/4$

The preceding limits may be exceeded for certain spins in which the model is difficult to control in the tunnel because of the high rate of descent or because of the wandering, oscillatory nature of the spin.

The accuracy of the measured weight and mass distribution of the models is believed to be within the following limits:

Weight, percent.....	$\pm 1$
Center-of-gravity location, percent $\bar{C}$ .....	$\pm 0.1$
Moments of inertia, percent.....	$\pm 0.5$

Control surface positions are set within  $\pm 1^\circ$  of stated values.

## References

1. Snow, W. L., Childers, B. A., Jones, S. B., and Fremaux, C. M.: "Recent Experiences with Implementing a Video Based Six Degree of Freedom Measurement System for Airplane Models in a 20-Foot Diameter Vertical Spin Tunnel," *Proceedings of the SPIE Videometrics Conference*, Volume 1820, 1992, pp. 158 - 180.
2. Scher, S. H. and White, W. L.: *Spin Tunnel Investigation of a 1/30-Scale Model of the McDonnell Douglas F/A-18 Airplane*. NASA TM SX-81809, 1980.
3. Wolowicz, C. H., Bowman, J. S., and Gilbert, W. P.: *Similitude Requirements and Scaling Relationships as Applied to Model Testing*, NASA TP 1435, 1979.
4. Chambers, J. R.: "Use of Dynamically Scaled Models for Studies of the High-Angle-of-Attack Behavior of Airplanes," presented at the International Symposium on Scale Modeling, Tokyo, Japan, July 18-22, 1988.
5. Neihouse, A. I.; Klinar, W. J.; and Scher, S. H.: *Status of Spin Research for Recent Airplane Designs*, NASA TR R-57, 1960. (supersedes NACA RM L57F12.)
6. Fremaux, C. M.: "Estimation of the Moment Coefficients for a Dynamically-Scaled, Free-Spinning Wind Tunnel Model," *Journal of Aircraft*, Volume 32, No. 6, 1995, pp. 1407 - 1409.

Table 1. Dimensional Characteristics of the F-18 HARV Airplane

Overall length, ft .....	56.0
Wing:	
Span (ref.), ft .....	37.42
Area (ref.), ft <sup>2</sup> .....	400.0
Root chord, in .....	190.29
Tip chord, in .....	66.28
Mean aerodynamic chord (projected), in .....	138.90
Aspect ratio .....	3.50
Taper ratio .....	0.35
Dihedral, deg .....	-3.0
Incidence, deg .....	0
Quarter-chord sweep, deg .....	20.0
Airfoil section:	
Root .....	modified NACA 65A; 5.0% thick
Intermediate.....	modified NACA 65A; 3.5% thick
Tip .....	modified NACA 65A; 3.5% thick
Aileron area (total), ft <sup>2</sup> .....	24.4
Leading-edge flap area (total), ft <sup>2</sup> .....	61.9
Trailing-edge flap area (total), ft <sup>2</sup> .....	48.4
Horizontal stabilators:	
Span (ref.), ft .....	14.67
Area (theoretical exposed), ft <sup>2</sup> .....	88.0
Root chord, in .....	98.70
Tip chord, in .....	45.45
Aspect ratio .....	2.44
Taper ratio .....	0.46
Dihedral, deg .....	-2
Quarter-chord sweep, deg .....	42.83
Airfoil section:	
Root .....	modified NACA 65A; 6% thick
Tip .....	modified NACA 65A; 2% thick
Vertical stabilizers:	
Height, in .....	95.0
Effective area (total for two tails), ft <sup>2</sup> .....	104.0
Aspect ratio .....	1.2
Taper ratio .....	0.40
Quarter-chord sweep, deg .....	35.0
Root chord, in .....	113.0
Tip chord, in .....	45.0
Cant angle, deg.....	20 outboard
Airfoil section:	
Root .....	modified NACA 65A; 5.0% thick
Tip .....	modified NACA 65A; 3.0% thick
Rudder area (total), ft <sup>2</sup> .....	15.4

Table 2. Dynamic Scaling Relationships used in Free Spin Testing

	Scale Factor
Linear dimension, $\ell$ .....	N
Relative density, $\mu$ ( $m/\rho\ell^3$ ).....	1
Froude number ( $V^2/\ell g$ ) .....	1
Weight, mass .....	$N^3/\sigma$
Moment of inertia .....	$N^5/\sigma$
Linear velocity .....	$N^{1/2}$
Linear acceleration.....	1
Angular velocity .....	$1/N^{1/2}$
Time .....	$N^{1/2}$
Reynolds number, $Re$ ( $V\ell/\nu$ ).....	$N^{3/2}\nu/\nu_0$

Model values are obtained by multiplying airplane values by the above scale factors, where N is the model-to-airplane scale ratio,  $\sigma$  is the ratio of air density at altitude to that at sea level ( $\rho/\rho_0$ ),  $\nu$  is the value of kinematic viscosity at altitude, and  $\nu_0$  is the value of kinematic viscosity at sea level.

Table 3. Mass Characteristics and Inertia Parameters of NASA F-18 HARV Airplane and Loading Tested on Model  
 [moments of inertia are given about the center of gravity]

Description	Weight, (lb)	Center-of-gravity location		Relative density, $\mu$ , at:		Moments of inertia (slug-ft <sup>2</sup> )			Mass properties			
		$x/\bar{c}$	$z/\bar{c}$	Sea Level	Altitude (25 000 ft)	$I_x$	$I_y$	$I_z$	IYMP	IRMP	IPMP	
												$x/\bar{c}$
Mass characteristics and inertia parameters of the airplane												
airplane	35 764	0.231	-0.039	31.13	67.53	22 632	174 246	189 336	-969 x 10 <sup>-4</sup>	-96 x 10 <sup>-4</sup>	1 066 x 10 <sup>-4</sup>	
Mass characteristics and inertia parameters of the model as-tested												
model as tested (vertical tails installed or removed)	35 393	0.232	-0.024	30.81	66.83	22 601	169 817	188 239	-951 x 10 <sup>-4</sup>	-119 x 10 <sup>-4</sup>	1 070 x 10 <sup>-4</sup>	

Table 4. Summary of Erect Spin and Spin-Recovery Characteristics of the Model with and without Vertical Tails Installed  
 [Values given are full-scale values converted from model-scale values]

Airplane: F-18 HARV		Attitude: erect	Direction of spin: pilot's left	Loading: 1	$\delta_f$ : 34D	Altitude: 25 000 ft			
Test no.	Spin block	Control surface deflection, deg			Status of vertical tails	Predicted equilibrium spin mode characteristics			
		For spin $\delta_r$	$\delta_a$	For recovery $\delta_d$		$^b \alpha$ , deg	$^c V$ , ft/s	$^c  \Omega $ , deg/s	Number of turns for recovery
1 4a, 5a, 6a		0	L25D R25U	L4U R24U	installed/ rudders neutral	90 [85] 80	285	154	2 1/4, 2 1/2
2 4b, 5b, 6b		30W	0		installed/ rudders actuated	91 [86] 82	285	159	1 1/2, 1 1/2
3 4c, 5c, 6c		N/A			removed	90 [85] 80	285	160	2 3/4, 2 3/4, 3

<sup>a</sup> figure numbers for corresponding  $\alpha$ ,  $\beta$ , and  $|\Omega|$  plots, respectively.

<sup>b</sup> range of angles shown are maximum and minimum measured values prior to input of recovery controls. Average values in [brackets].

<sup>c</sup> average value obtained prior to input of recovery controls.

Table 5. Summary of Inverted Spin and Spin-Recovery Characteristics of the Model with and without Vertical Tails Installed  
 [Values given are full-scale values converted from model-scale values]

Airplane: F-18 HARV		Attitude: inverted		Direction of spin: pilot's left		Loading: 1		δf: 0		Altitude: 25 000 ft	
Test no.	Spin block	Control surface deflection, deg				Status of vertical tails	Predicted equilibrium spin mode characteristics			Number of turns for recovery	
		For spin δ <sub>r</sub>	δ <sub>a</sub>	For recovery δ <sub>d</sub>			<sup>b</sup> α, deg	<sup>b</sup> β, deg	<sup>c</sup> V, ft/s		<sup>c</sup>  Ω , deg/s
4 7a, 8a, 9a		0	L25U R25D	---	L10U R10D	installed/ rudders neutral	---	---	---	---	<sup>d</sup> no spin
5 7b, 8b, 9b		30W	L25U R25D	L0 R0	L10U R10D	installed/ rudders actuated	-84 [-77]	40 [1]	305	99	2
6 7c, 8c, 9c		N/A	L25U R25D	L0 R0	L10U R10D	removed	-90 [-82]	11 [-1]	295	111	4 1/4, 4 1/4, 4 1/2
7 7d, 8d, 9d		N/A	L25U R25D	L25D R25U	L10U R10D	removed	-90 [-83]	9 [-2]	295	119	1 1/2, 1 3/4

<sup>a</sup> figure numbers for corresponding α, β, and |Ω| plots, respectively.  
<sup>b</sup> range of angles shown are maximum and minimum measured values prior to input of recovery controls. Average values in [brackets].  
<sup>c</sup> average value obtained prior to input of recovery controls.  
<sup>d</sup> model oscillated out of spin several turns after launch.

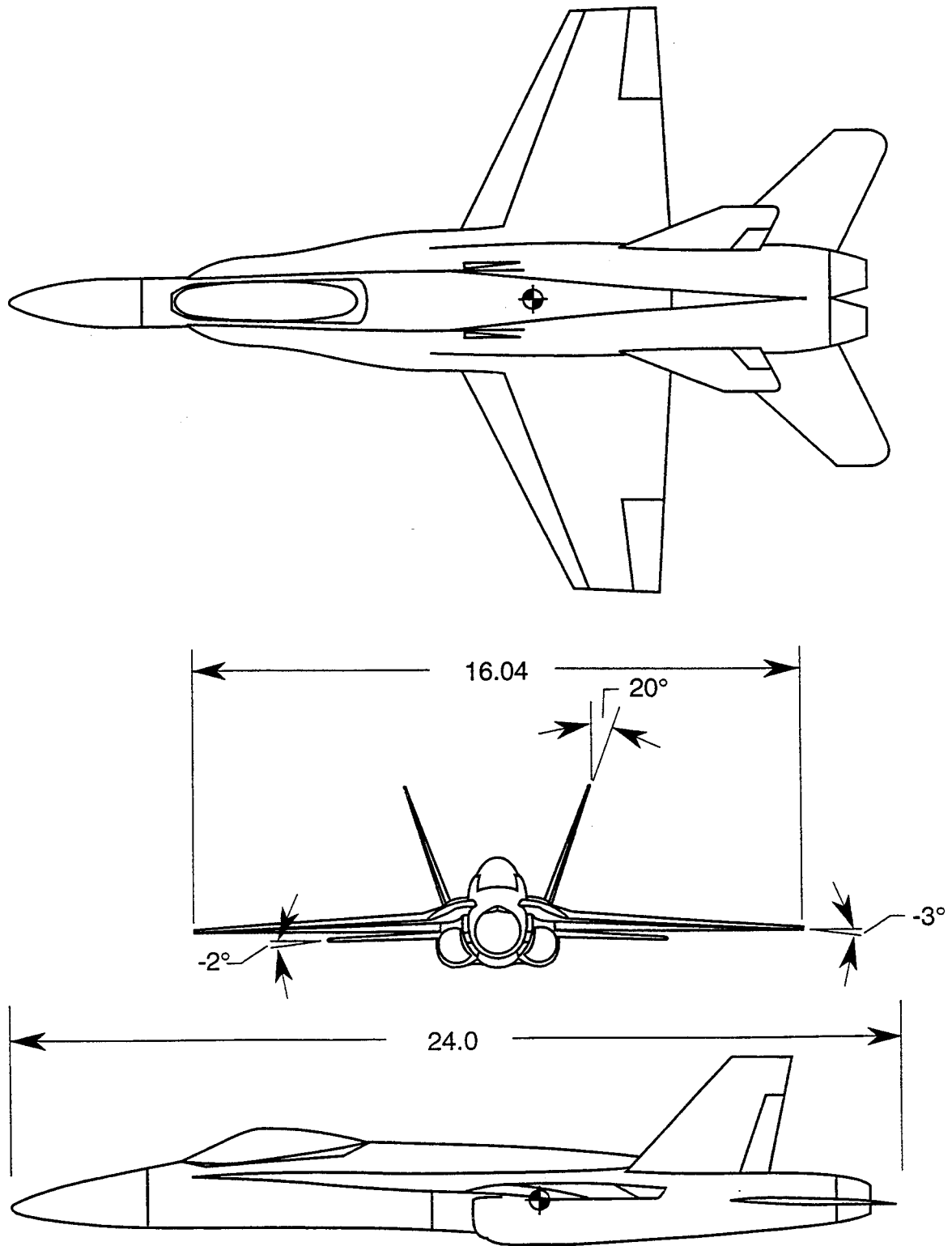


Figure 1. Three-view drawing of unmodified 1/28-scale free-spin model of NASA F-18 HARV airplane. Center of gravity position shown is  $0.234\bar{c}$ . Dimensions are in inches.

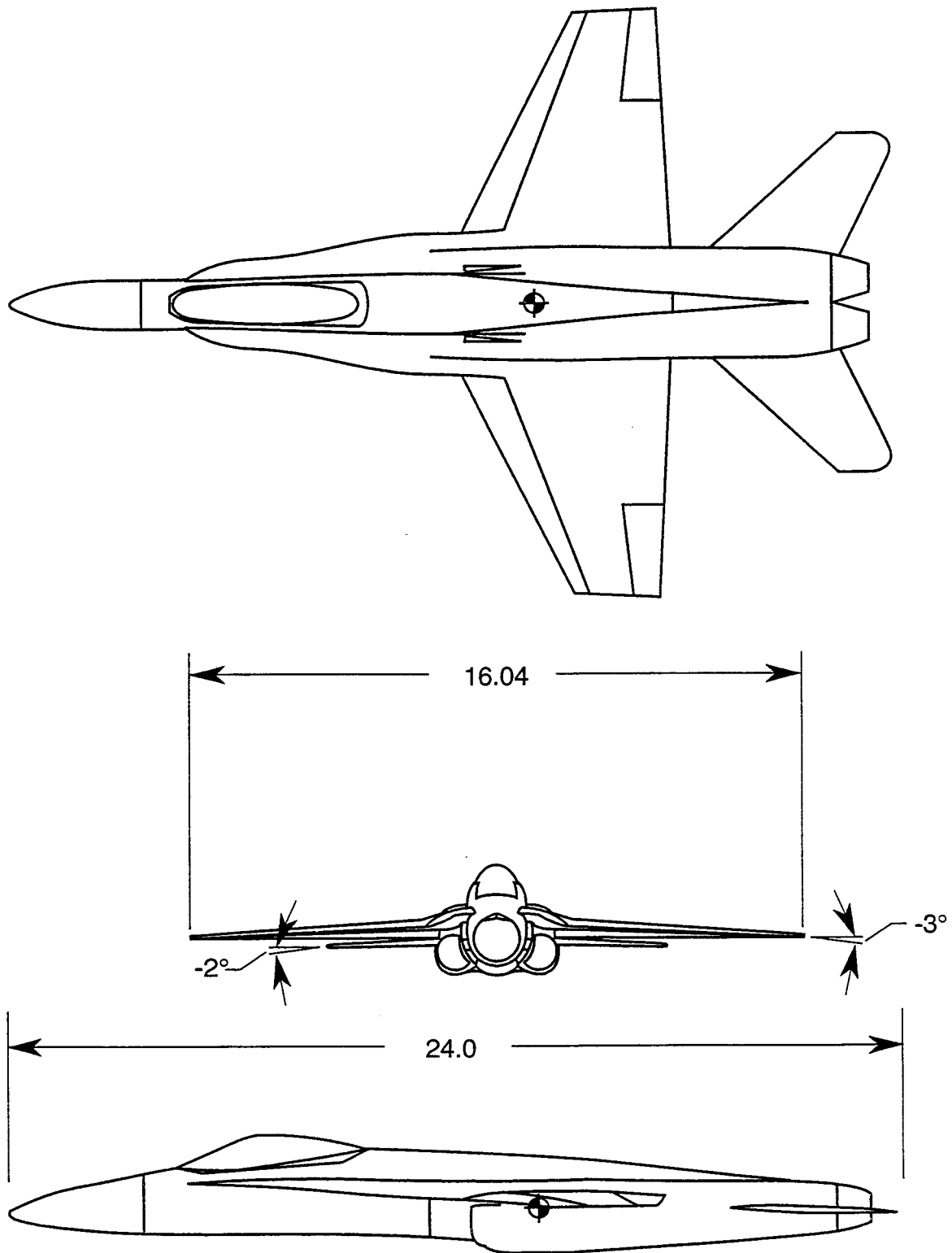
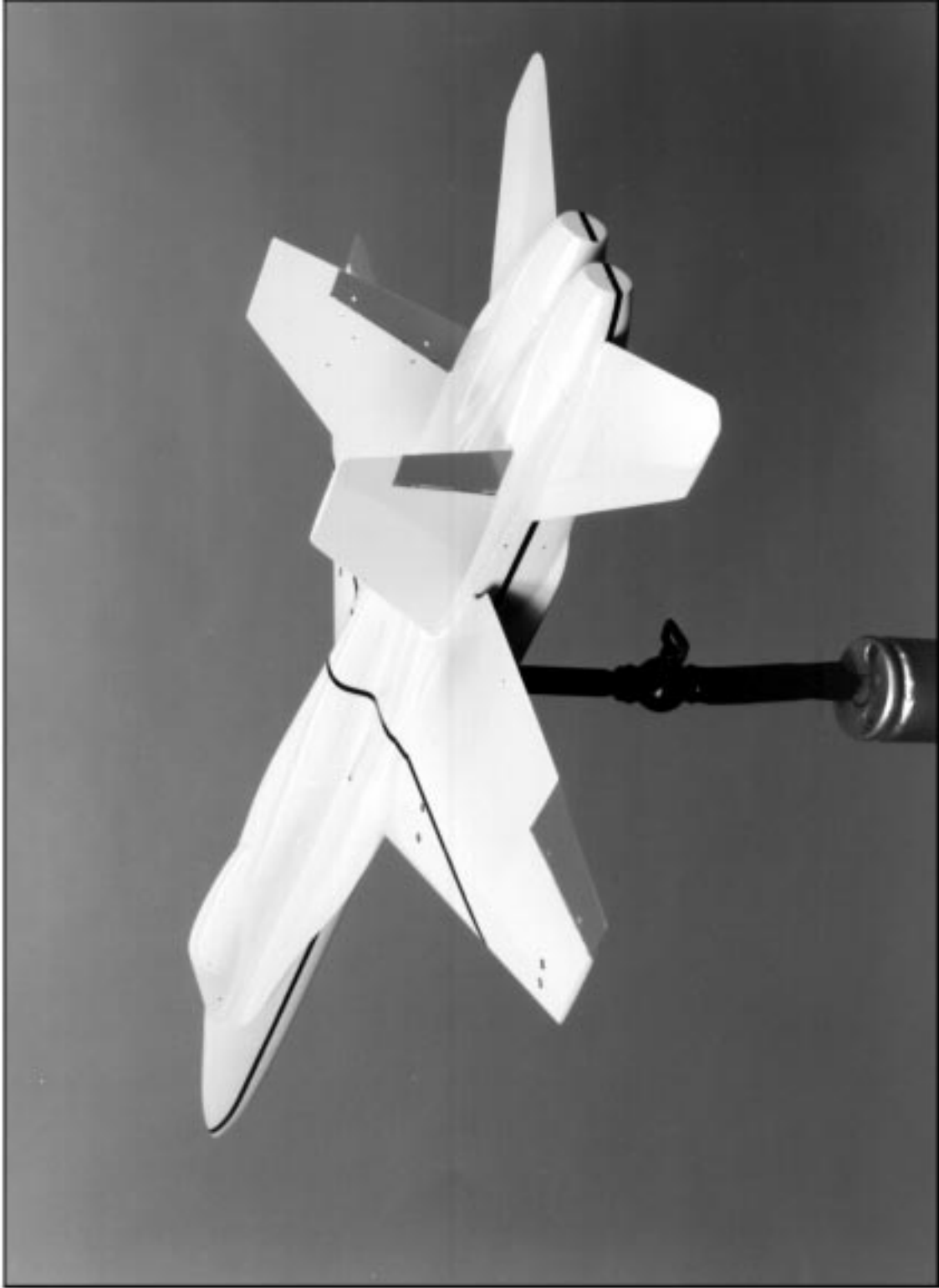


Figure 2. Three-view drawing of modified 1/28-scale free-spin model of NASA F-18 HARV airplane with vertical tails removed. Center of gravity position shown is  $0.234\bar{c}$ . Dimensions are in inches.



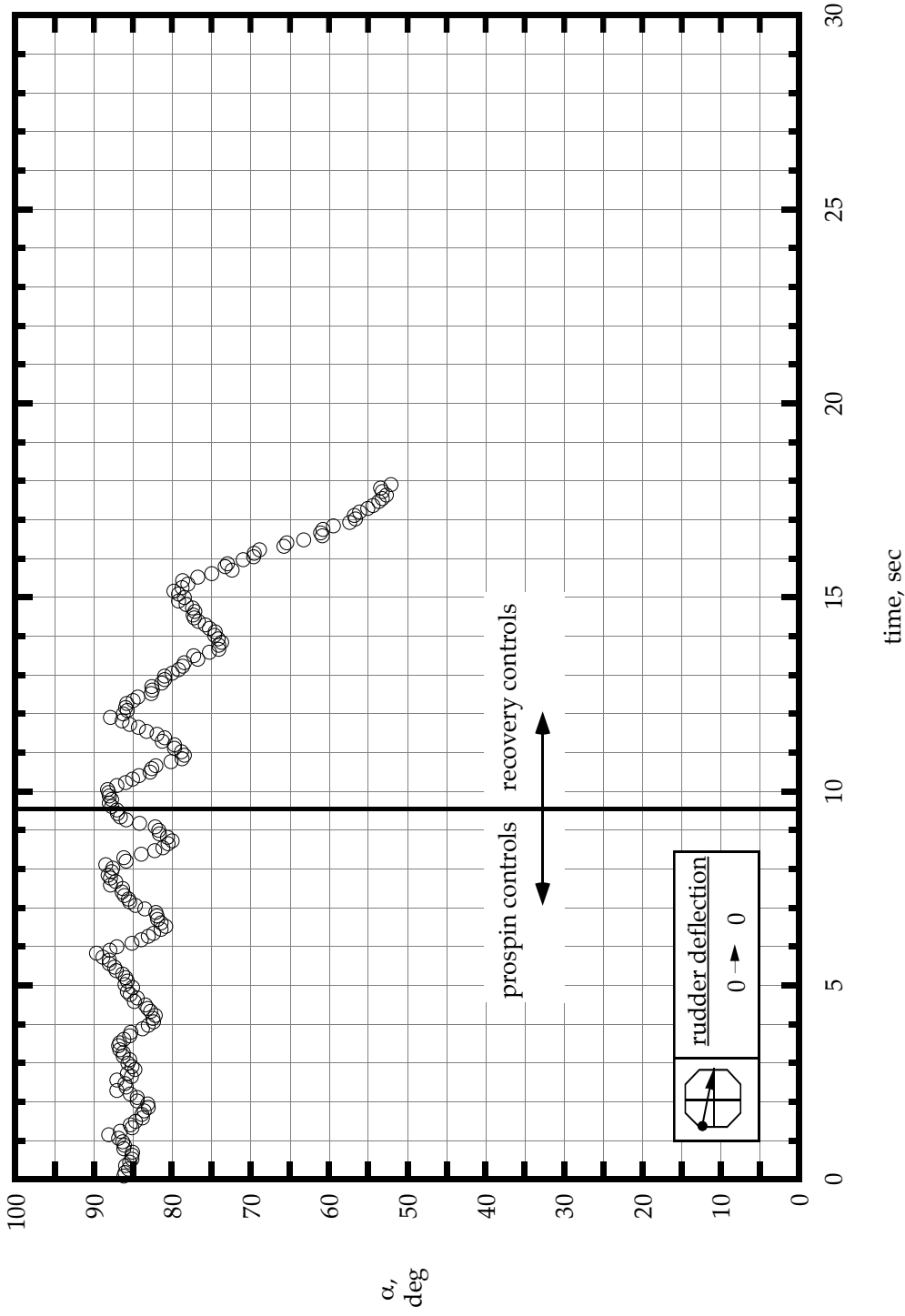
(a) front view from the right

Figure 3. 1/28-scale F-18 HARV model.



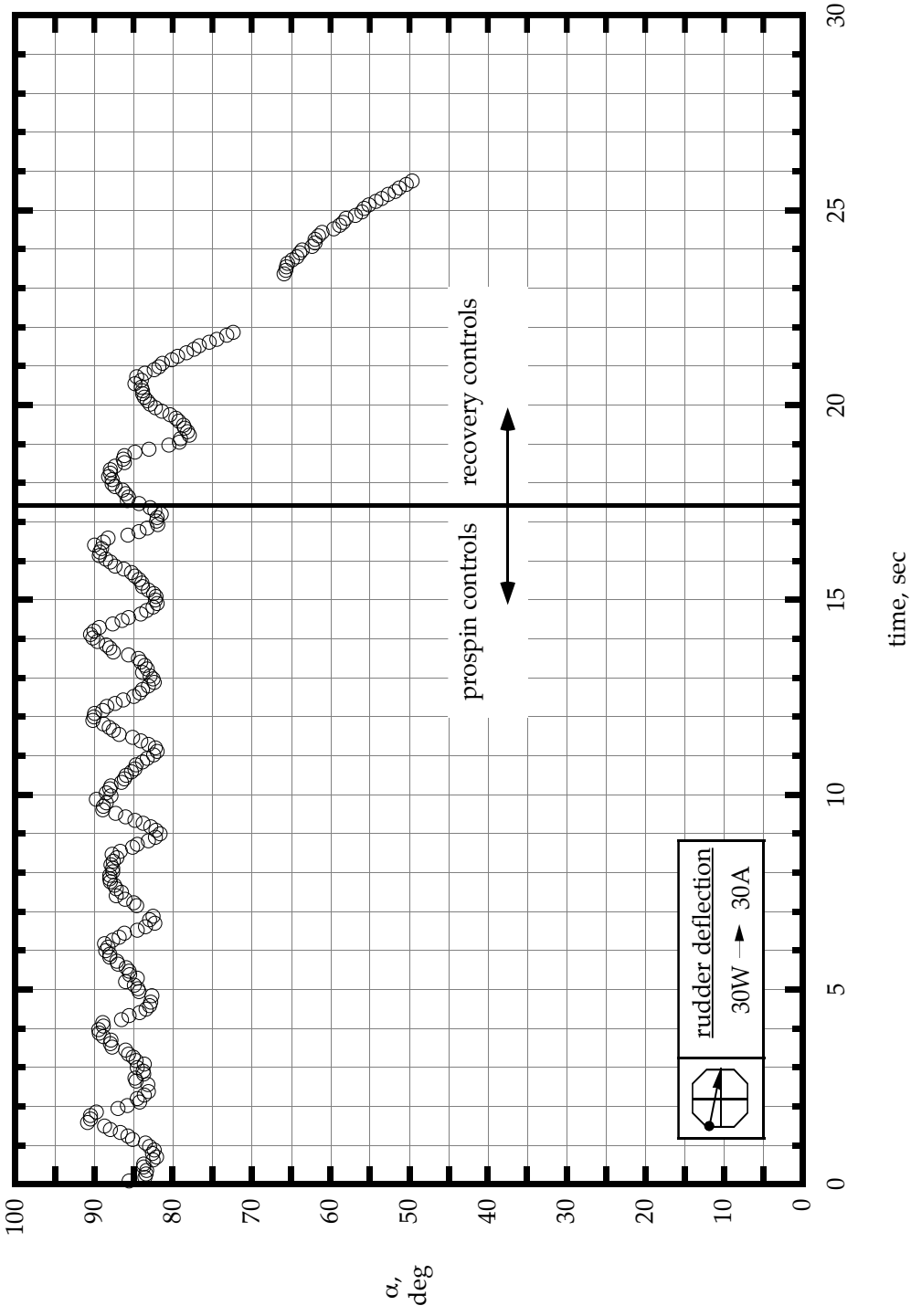
(b) rear view from the left

Figure 3. Concluded.



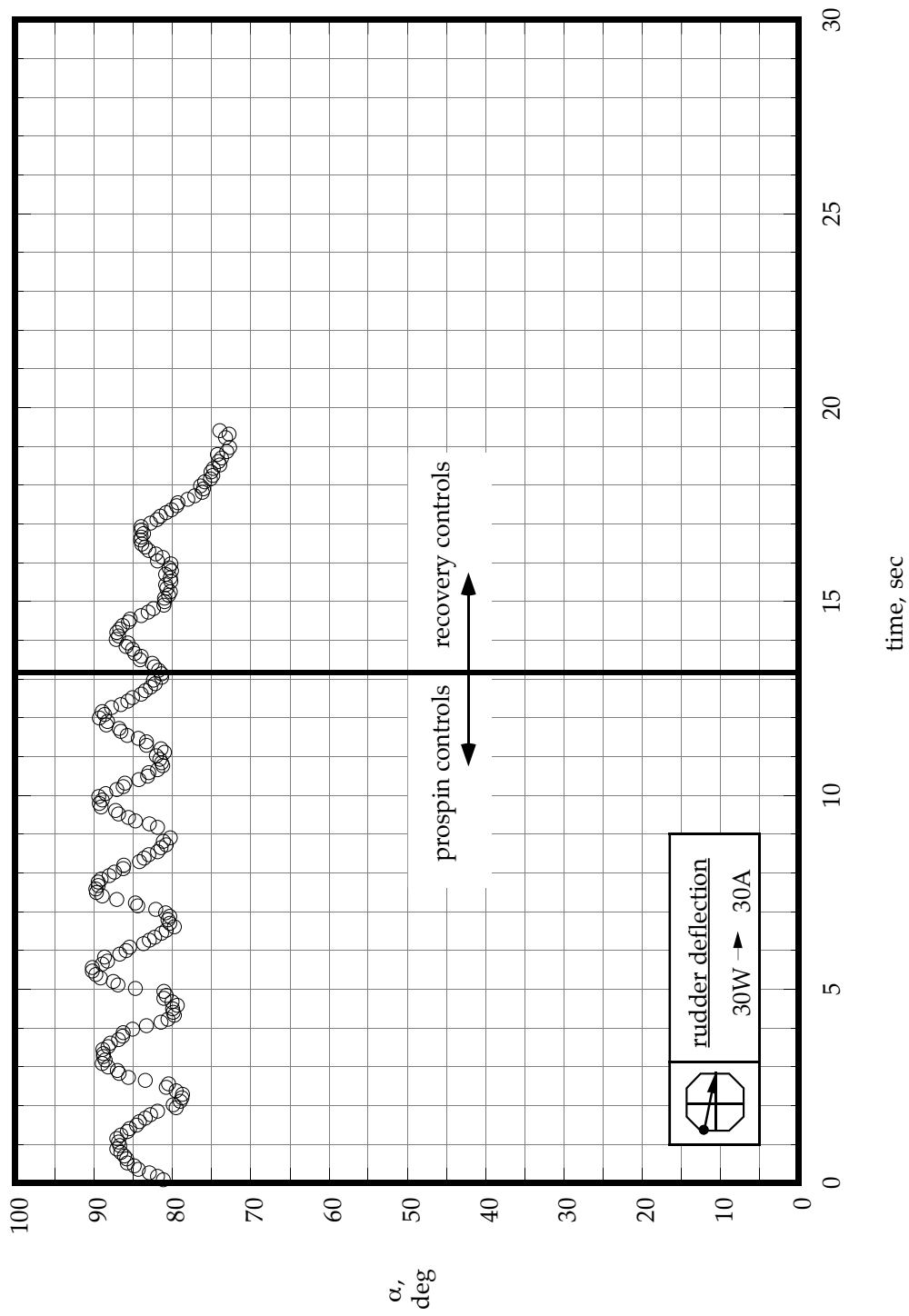
(a) vertical tails installed - rudders neutral (see test 1 - table 4).

Figure 4. Angle of attack during erect spin tests of the model. Values shown are full-scale values converted from model-scale values.



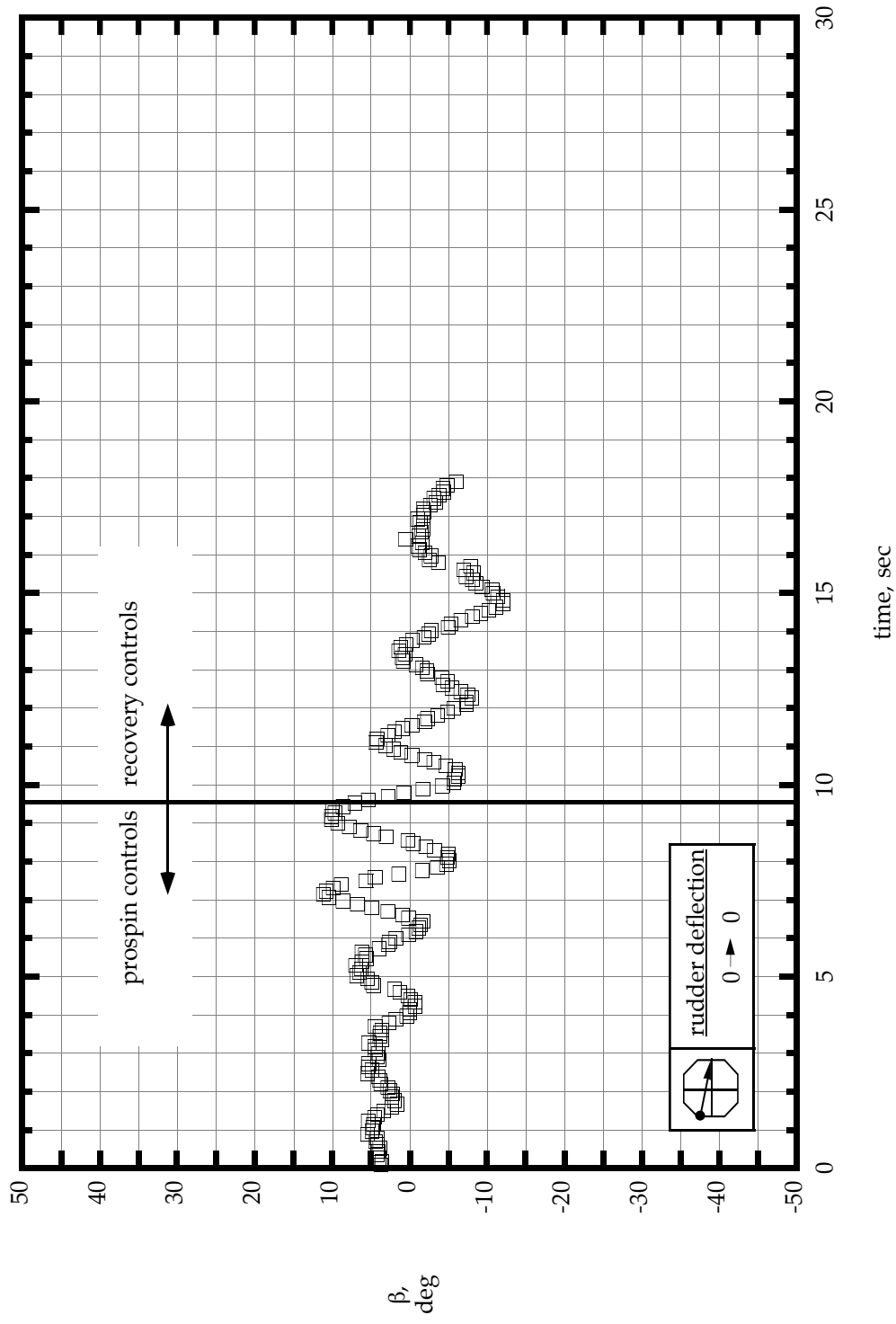
(b) vertical tails installed - rudders actuated (see test 2 - table 4).

Figure 4. Continued.



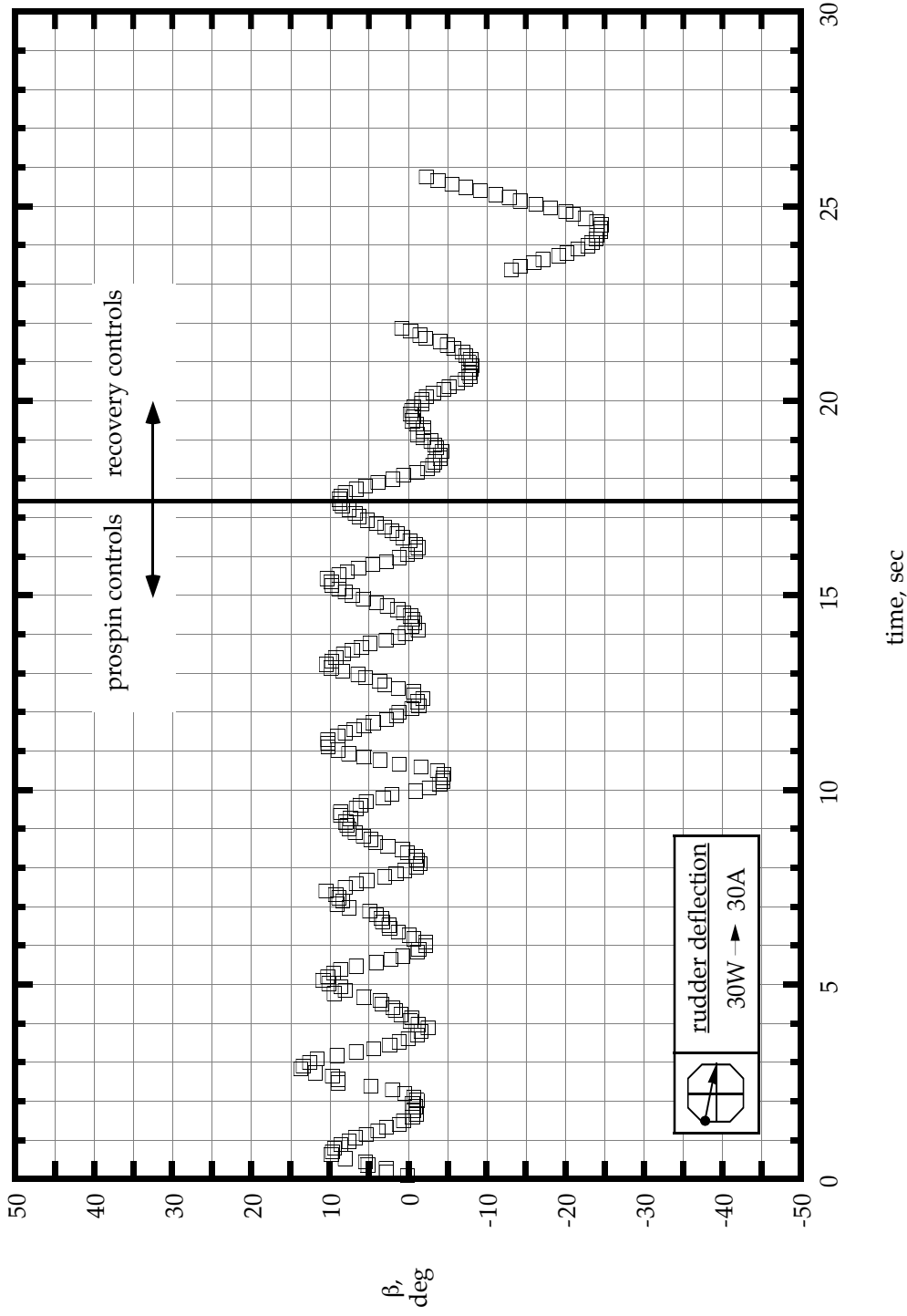
(c) vertical tails removed (see test 3 - table 4).

Figure 4. Concluded.



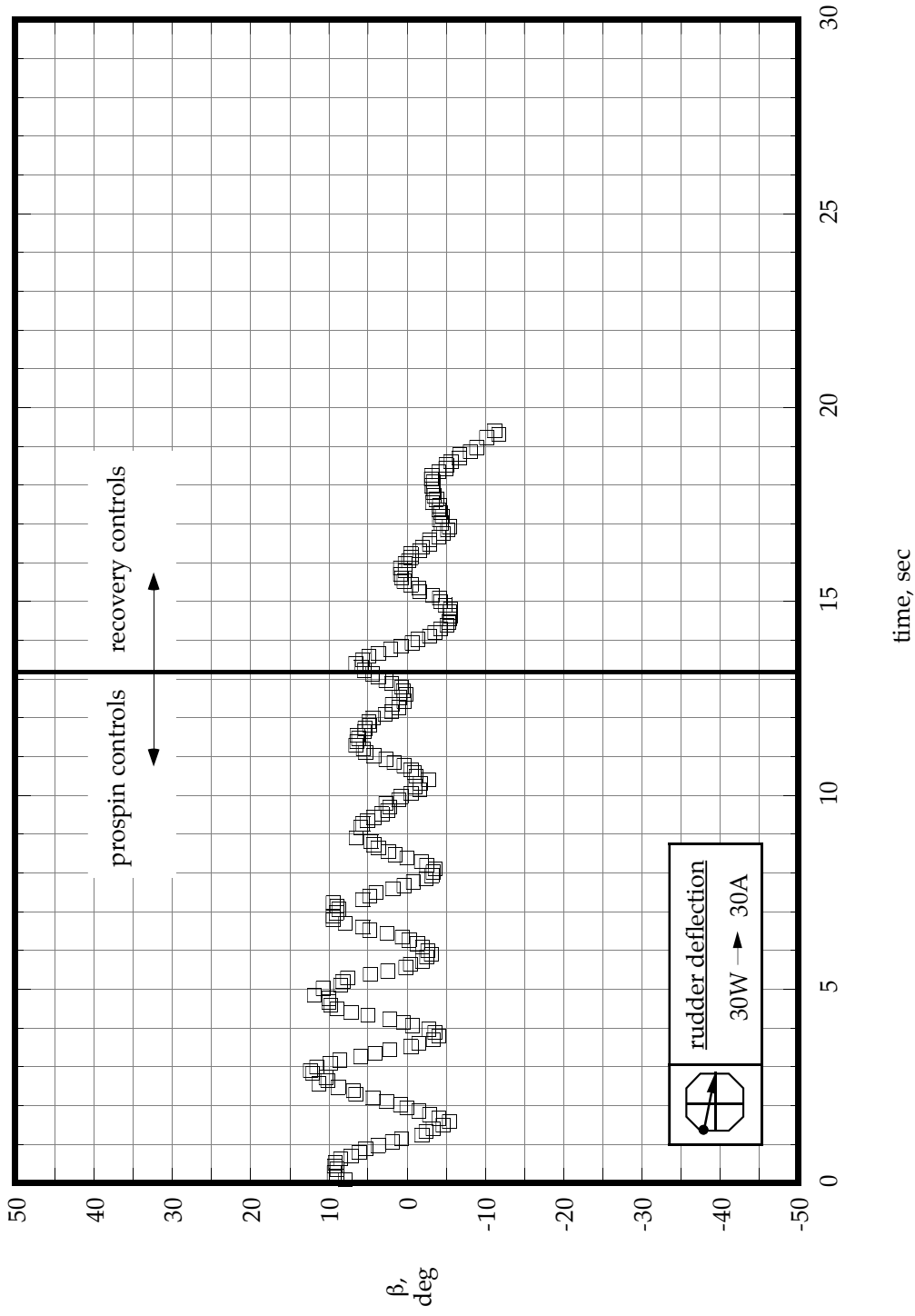
(a) vertical tails installed- rudders neutral (see test 1 - table 4).

Figure 5. Sideslip angle during erect spin tests of the model. Values shown are full-scale values converted from model-scale values.



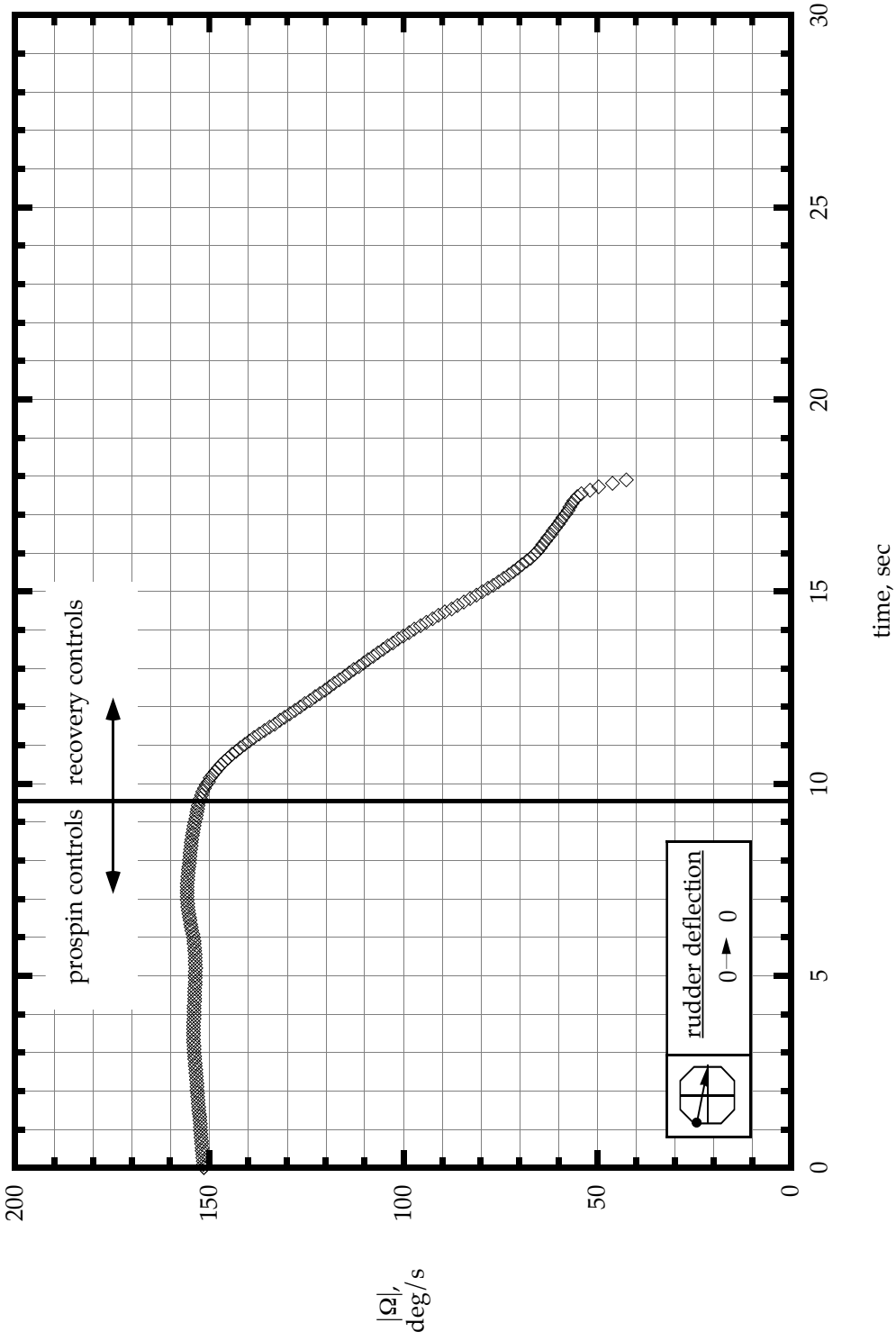
(b) vertical tails installed- rudders actuated (see test 2 - table 4).

Figure 5. Continued.



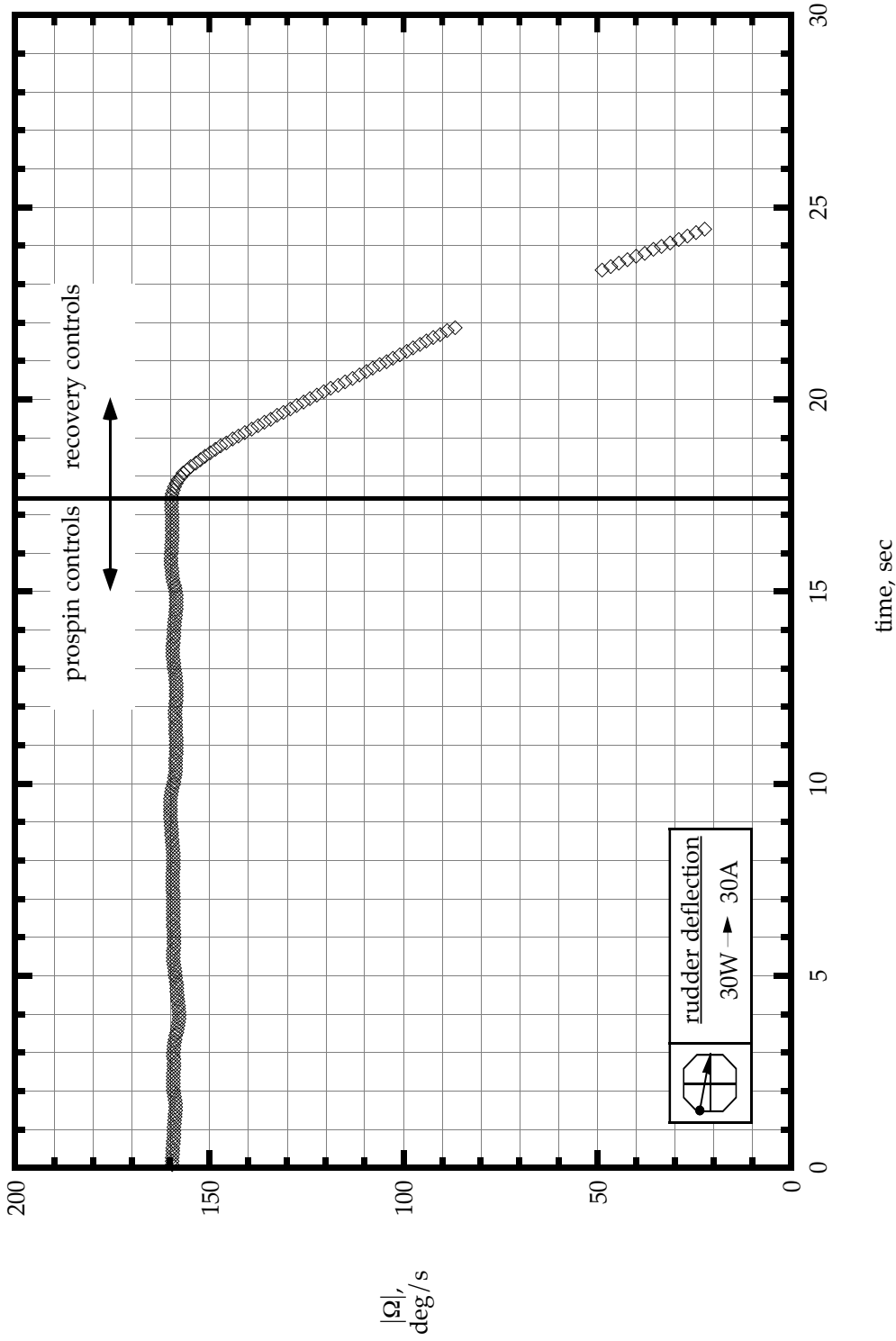
(c) vertical tails removed (see test 3 - table 4).

Figure 5. Concluded.



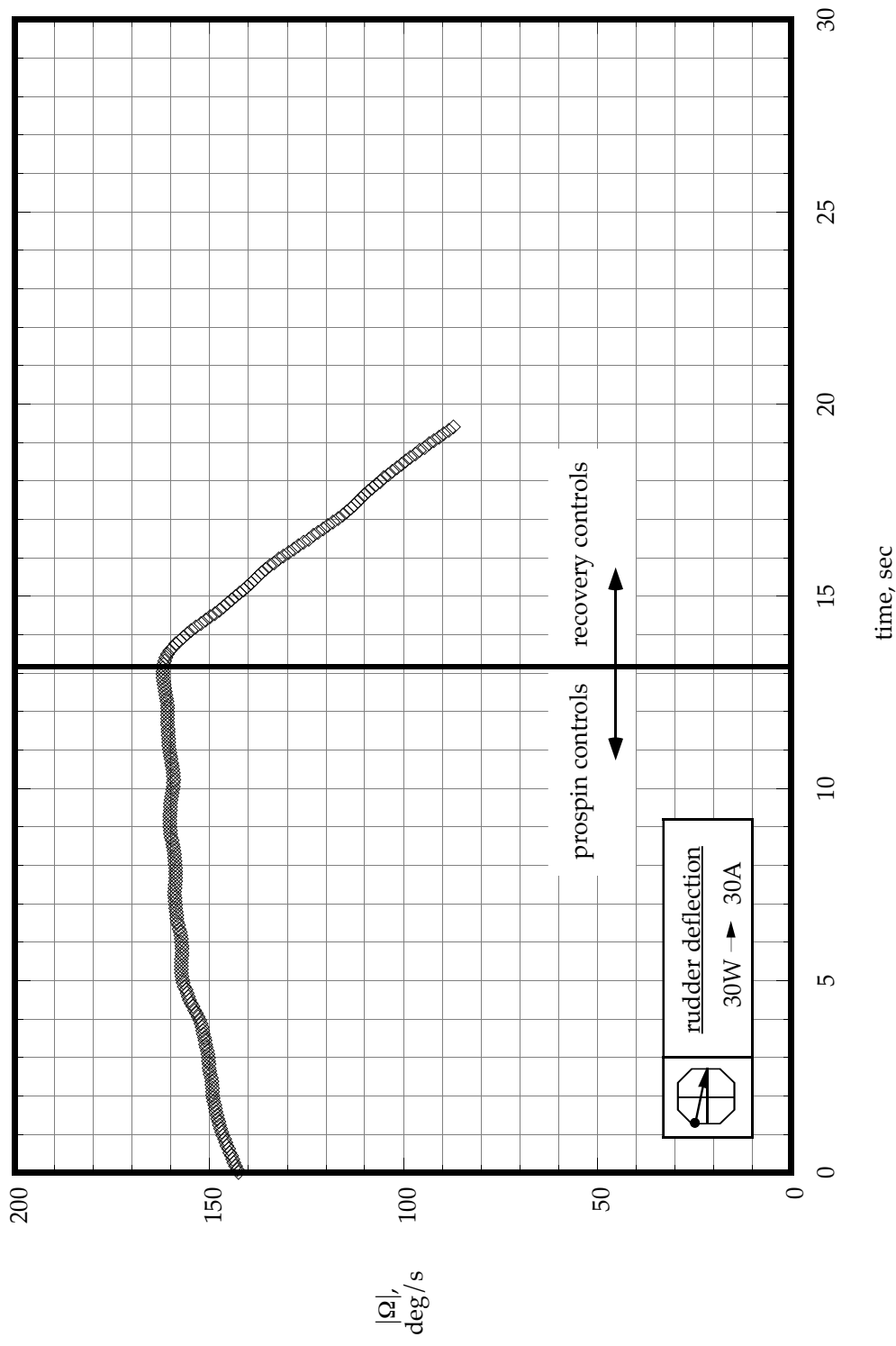
(a) vertical tails installed- rudders neutral (see test 1 - table 4).

Figure 6. Magnitude of spin rate during erect spin tests of the model. Values shown are full-scale values converted from model-scale values.



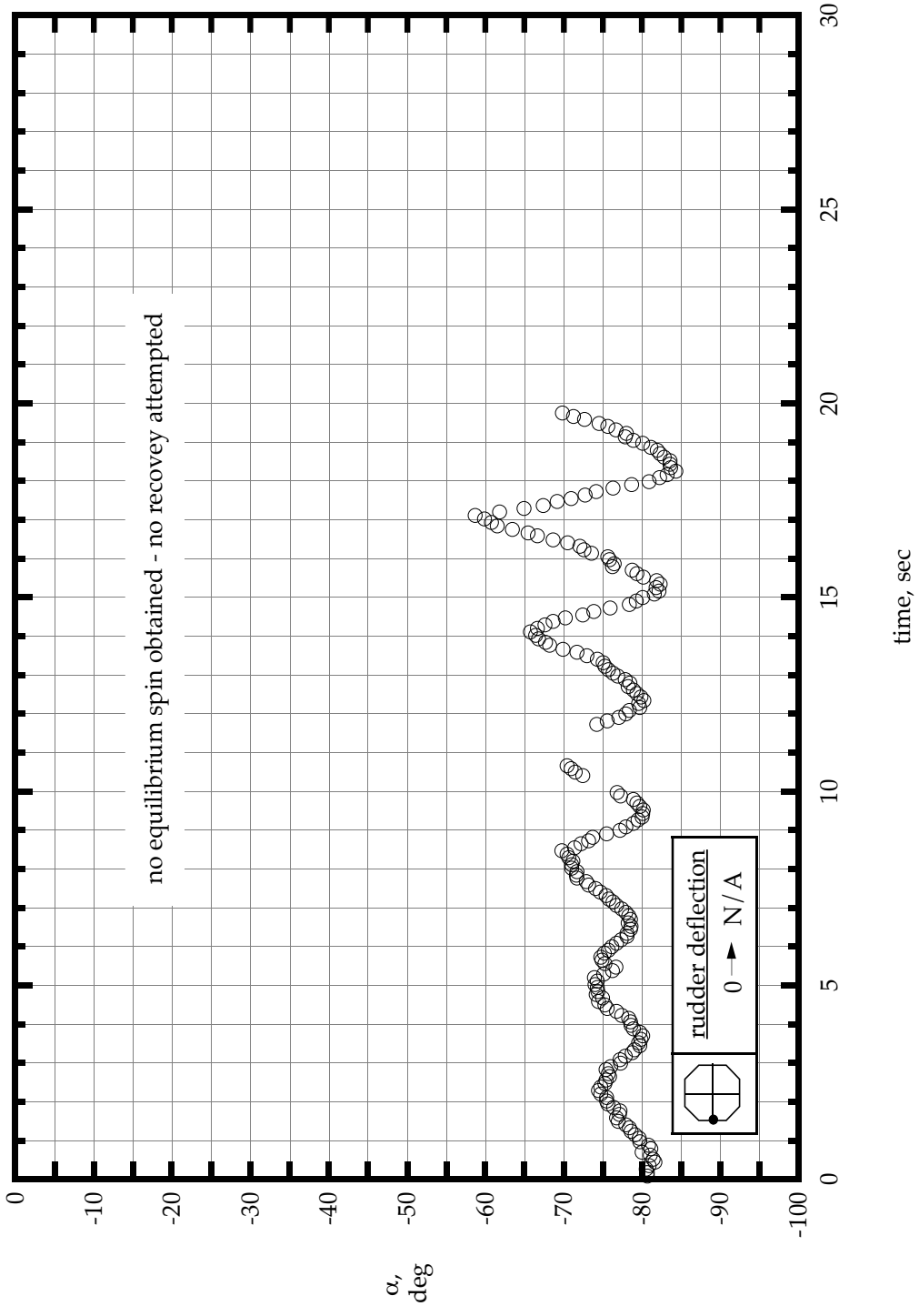
(b) vertical tails installed- rudders actuated (see test 2 - table 4).

Figure 6. Continued.



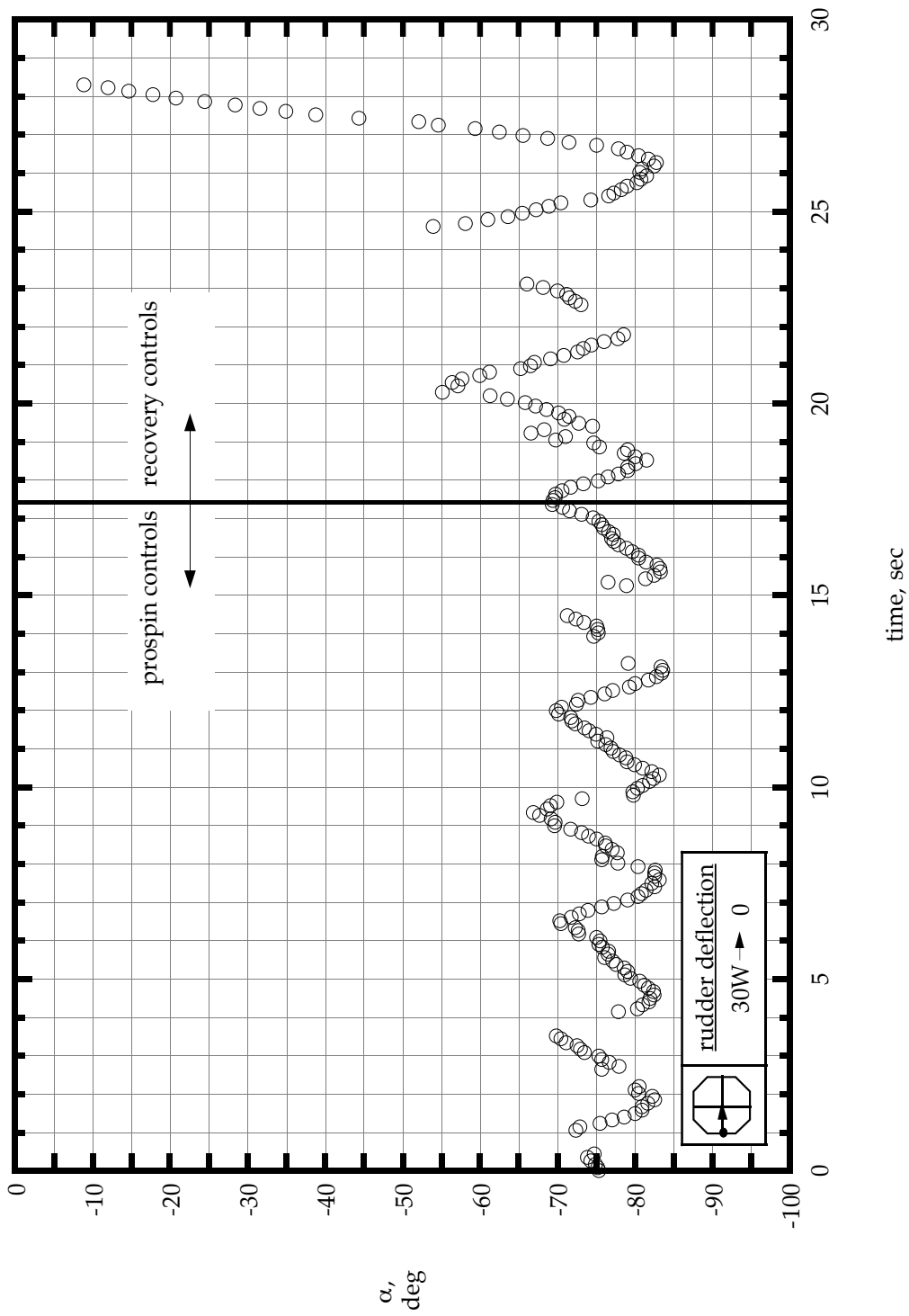
(c) vertical tails removed (see test 3 - table 4).

Figure 6. Concluded.



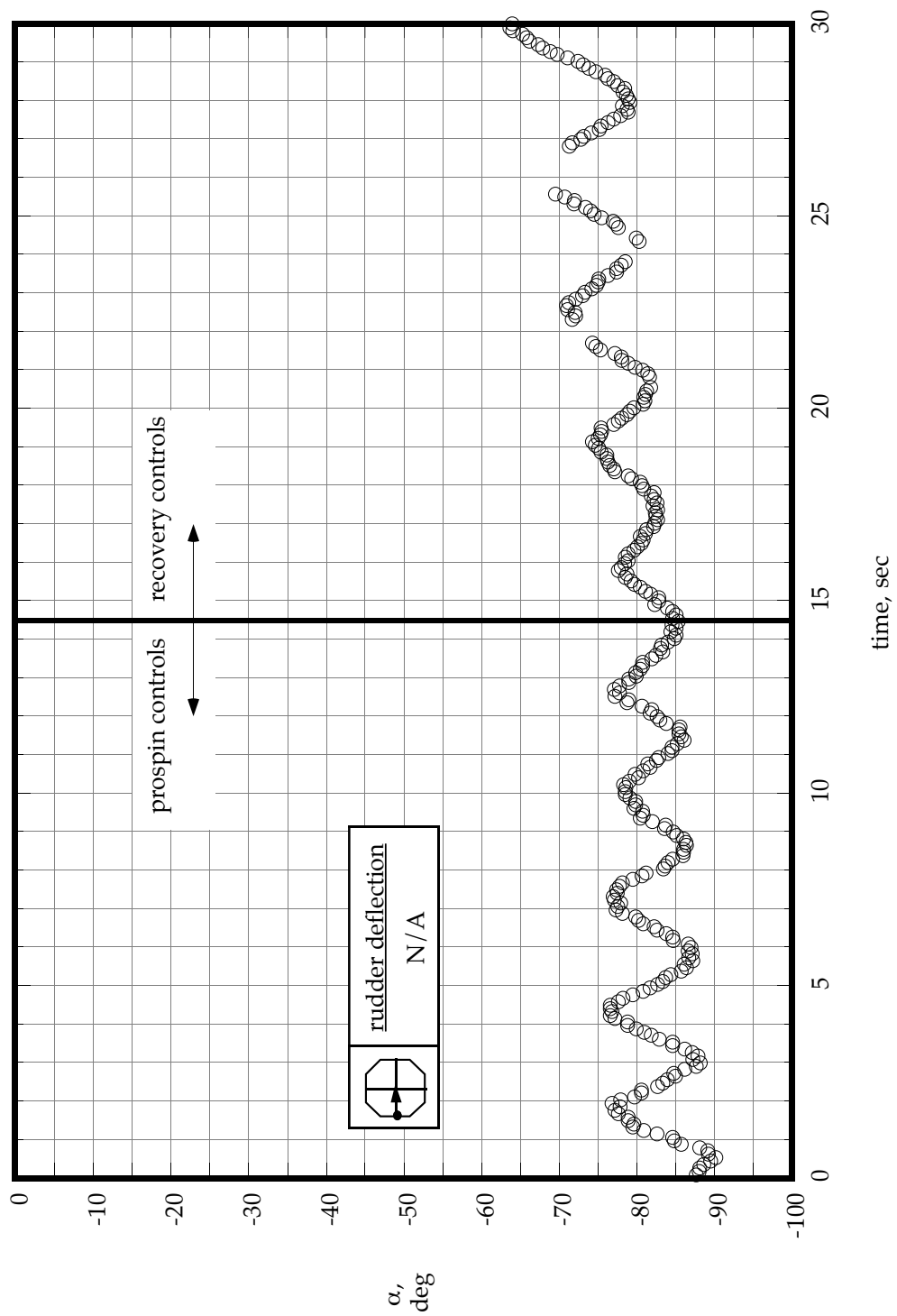
(a) vertical tails installed- rudders neutral (see test 4 - table 5).

Figure 7. Angle of attack during inverted spin tests of the model. Values shown are full-scale values converted from model-scale values.



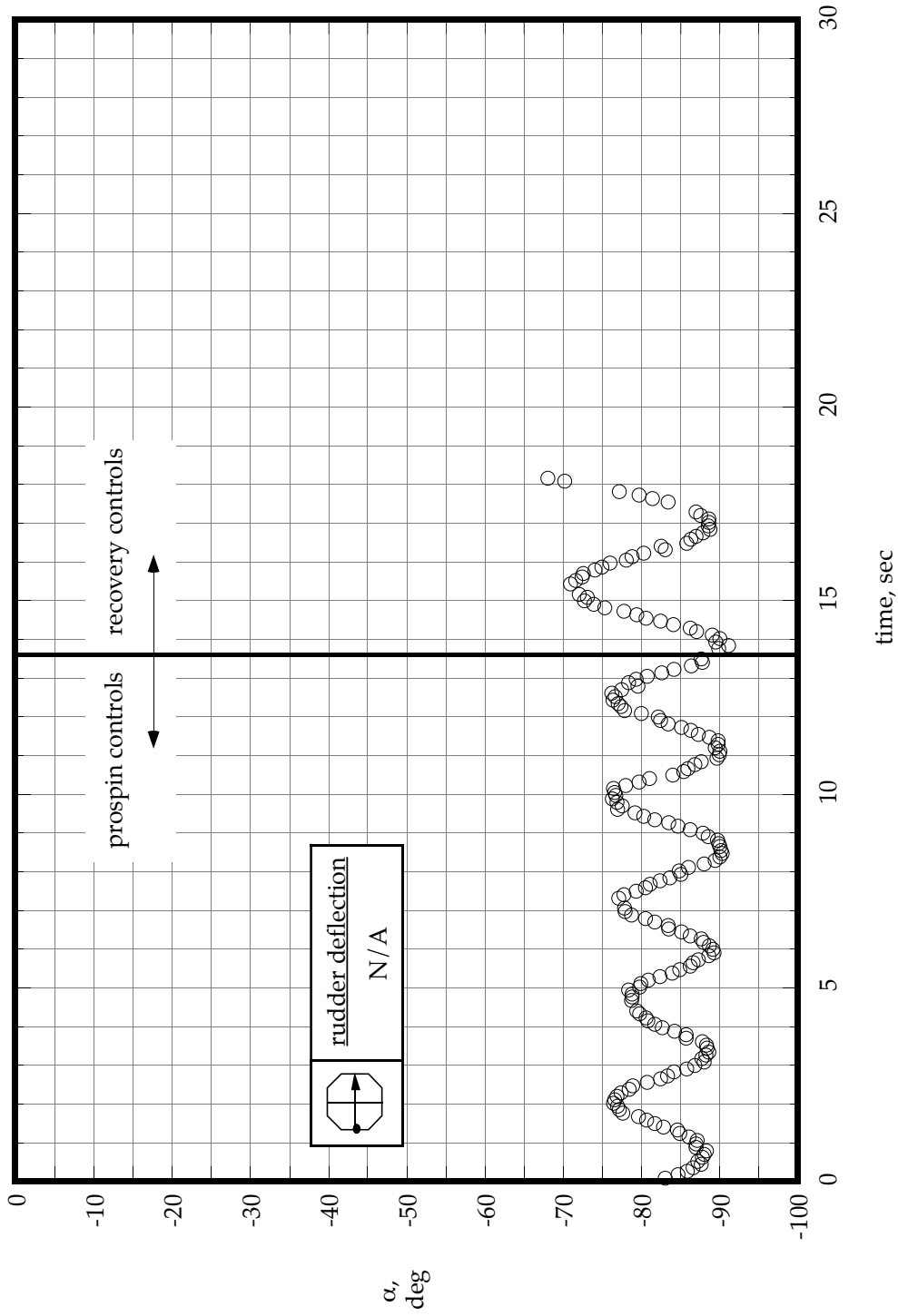
(b) vertical tails installed - rudders actuated (see test 5 - table 5).

Figure 7. Continued.



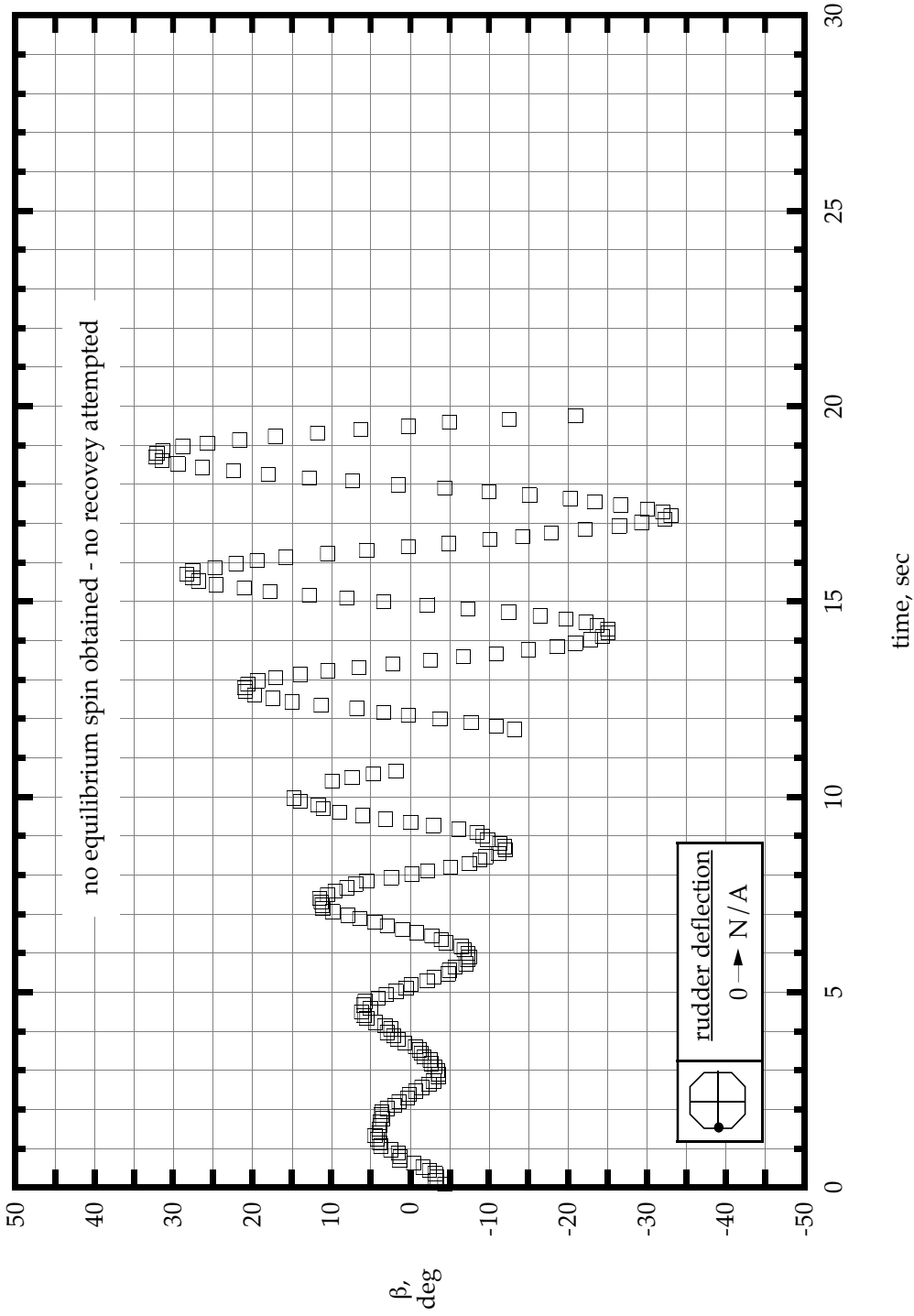
(c) vertical tails removed (see test 6 - table 5).

Figure 7. Continued.



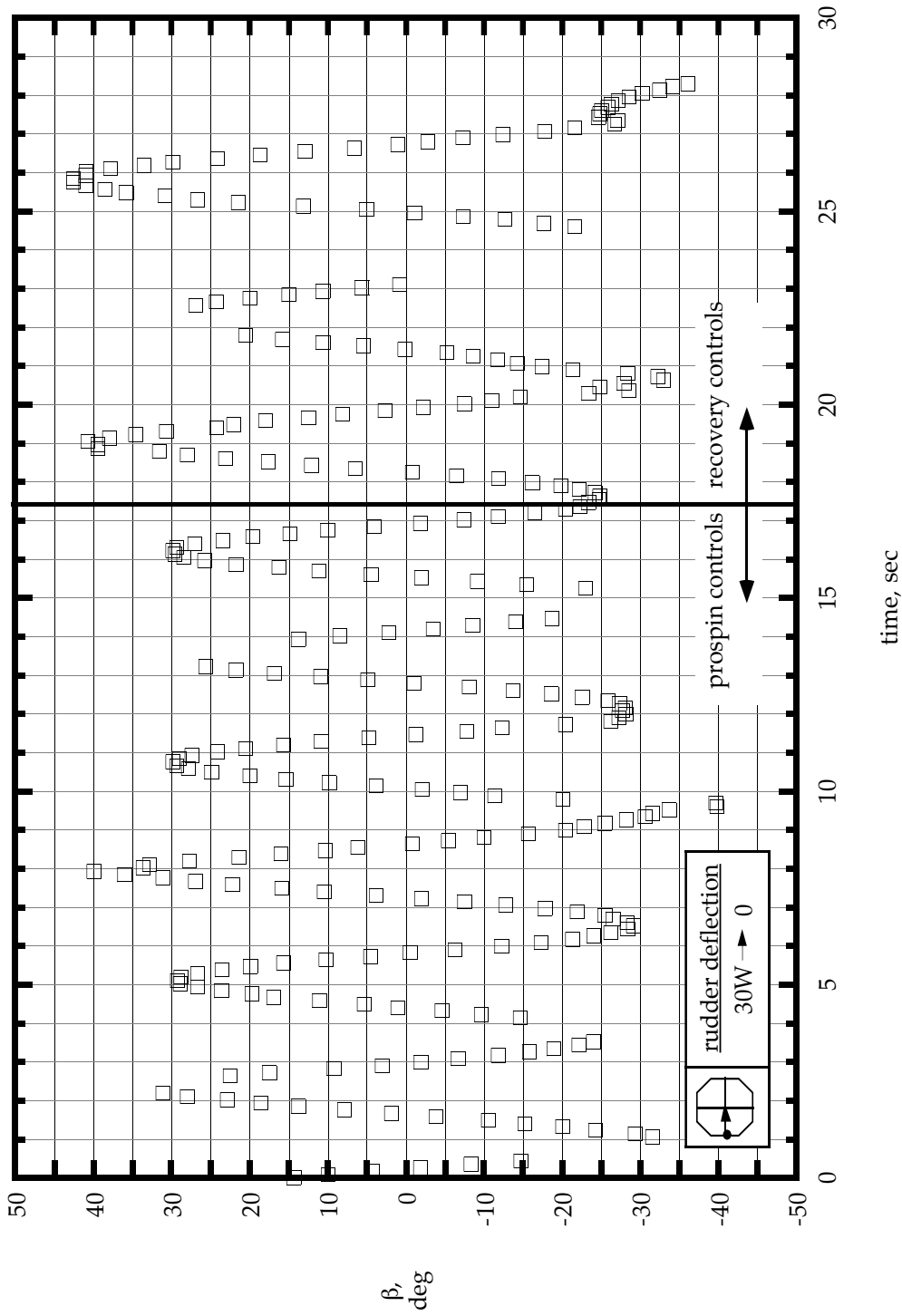
(d) vertical tails removed - lateral controls with spin for recovery (see test 7 - table 5).

Figure 7. Concluded.



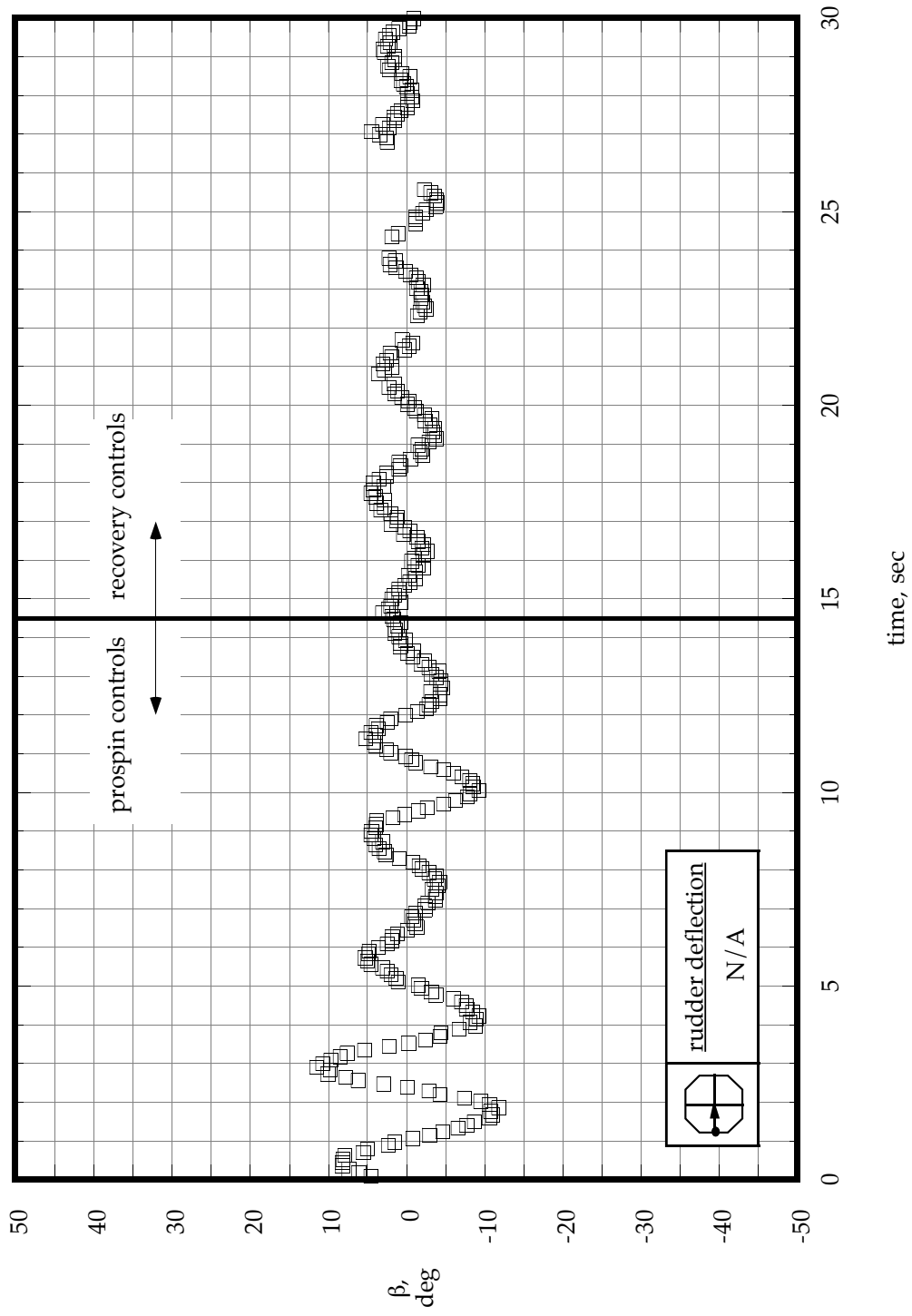
(a) vertical tails installed - rudders neutral (see test 4 - table 5).

Figure 8. Sideslip angle during inverted spin tests of the model. Values shown are full-scale values converted from model-scale values.



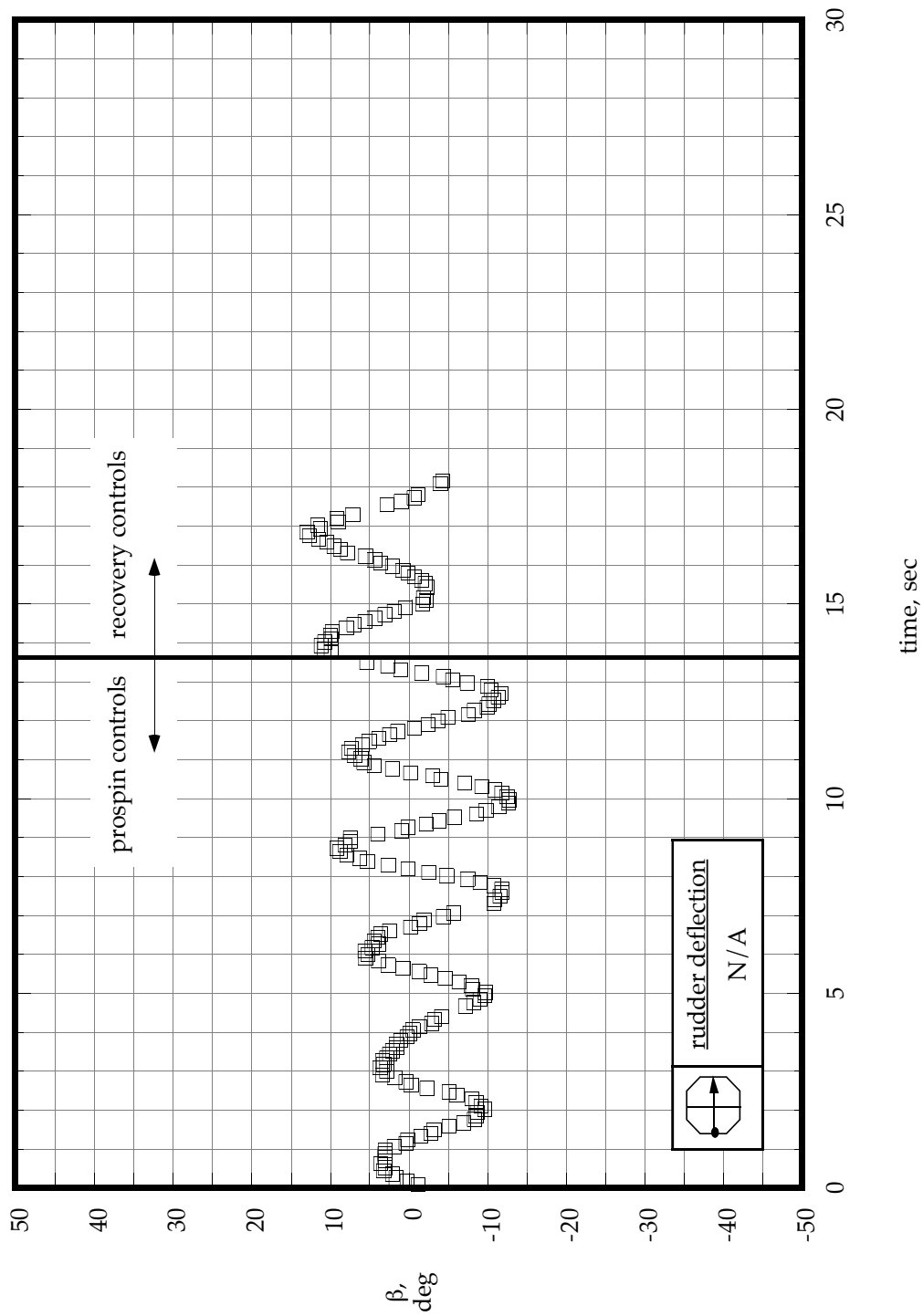
(b) vertical tails installed - rudders actuated (see test 5 - table 5).

Figure 8. Continued.



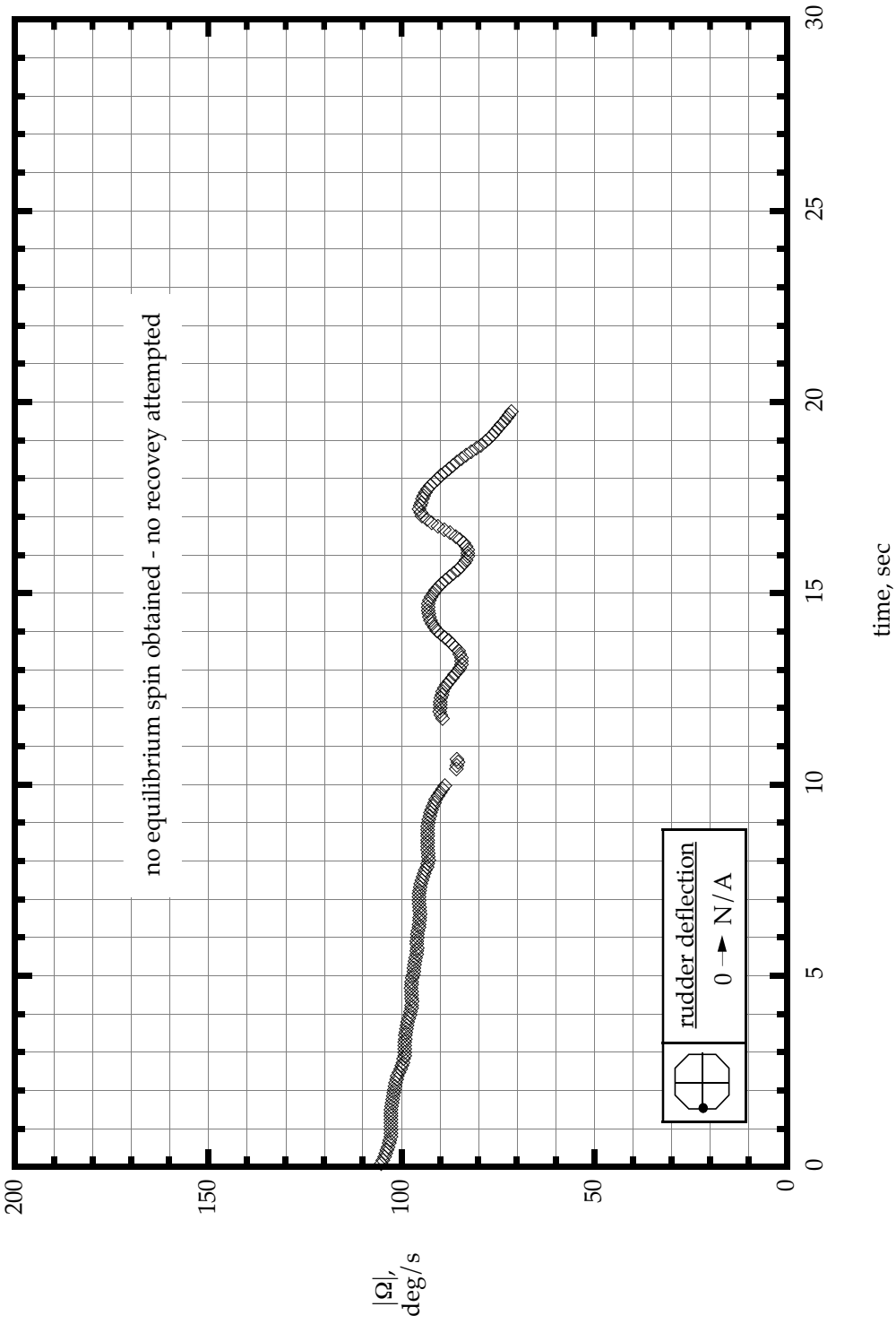
(c) vertical tails removed (see test 6 - table 5).

Figure 8. Continued.



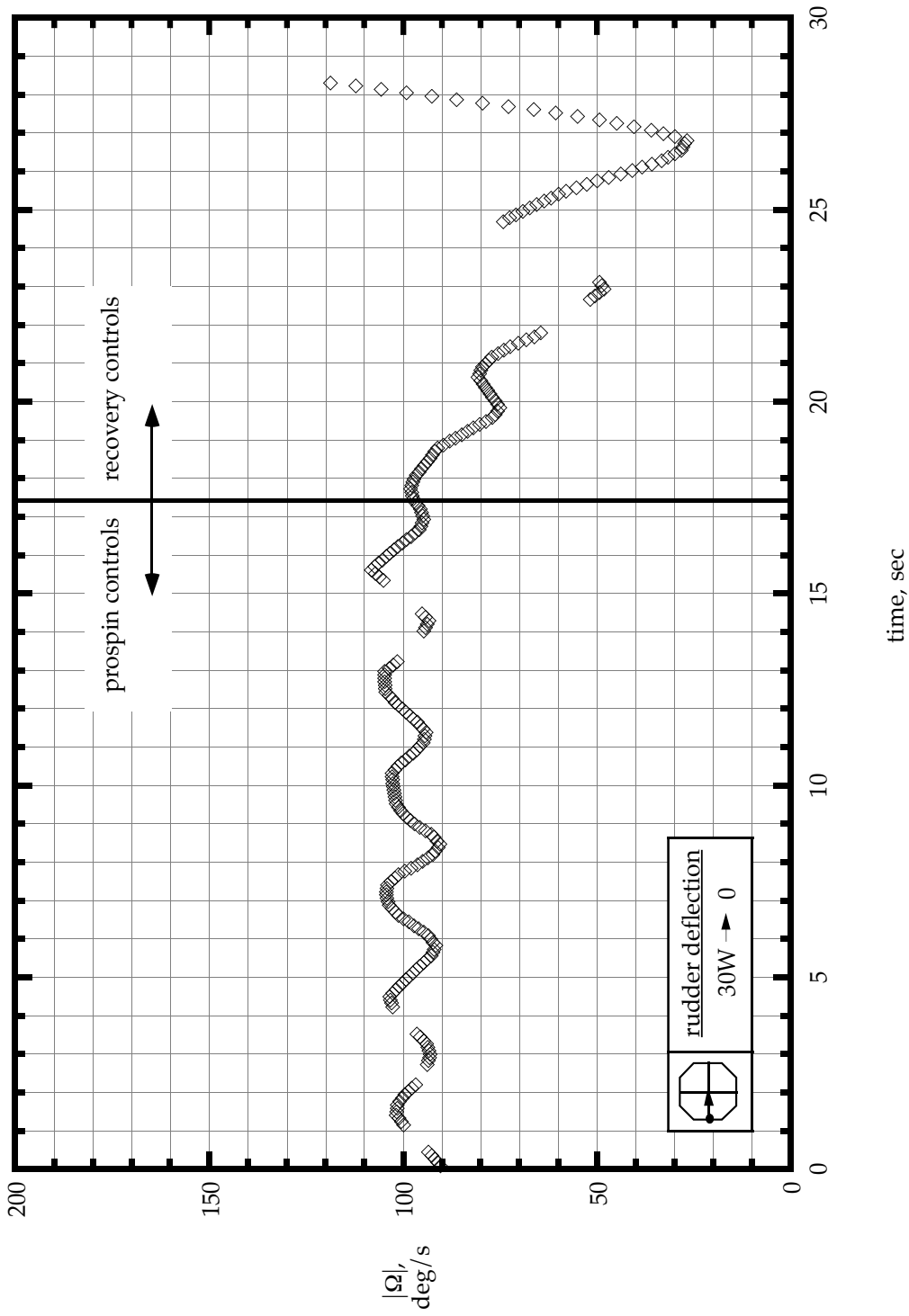
(d) vertical tails removed - lateral controls with spin for recovery (see test 7 - table 5).

Figure 8. Concluded.



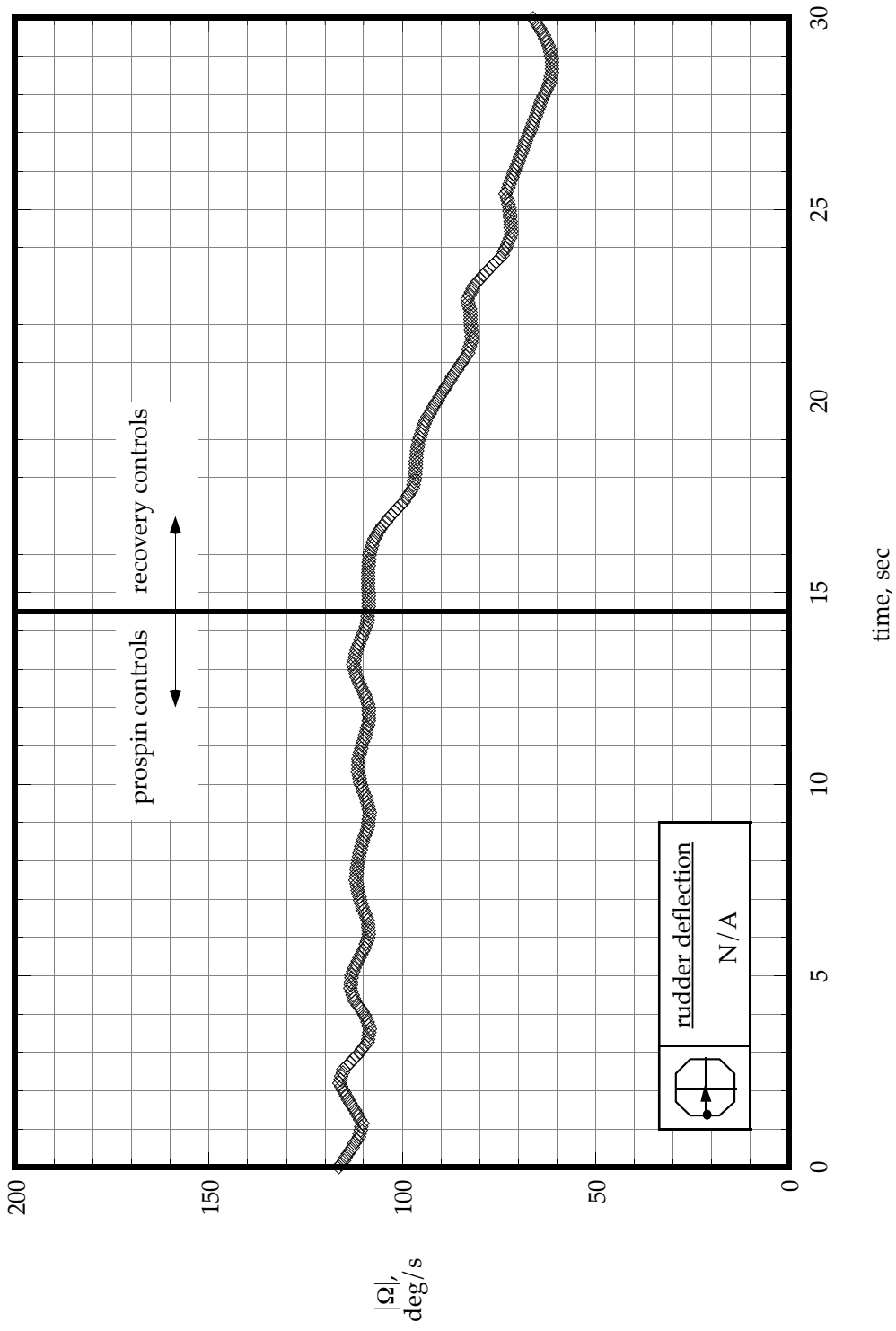
(a) vertical tails installed- rudders neutral (see test 4 - table 5).

Figure 9. Magnitude of spin rate for inverted spin tests of the model. Values shown are full-scale values converted from model-scale values.



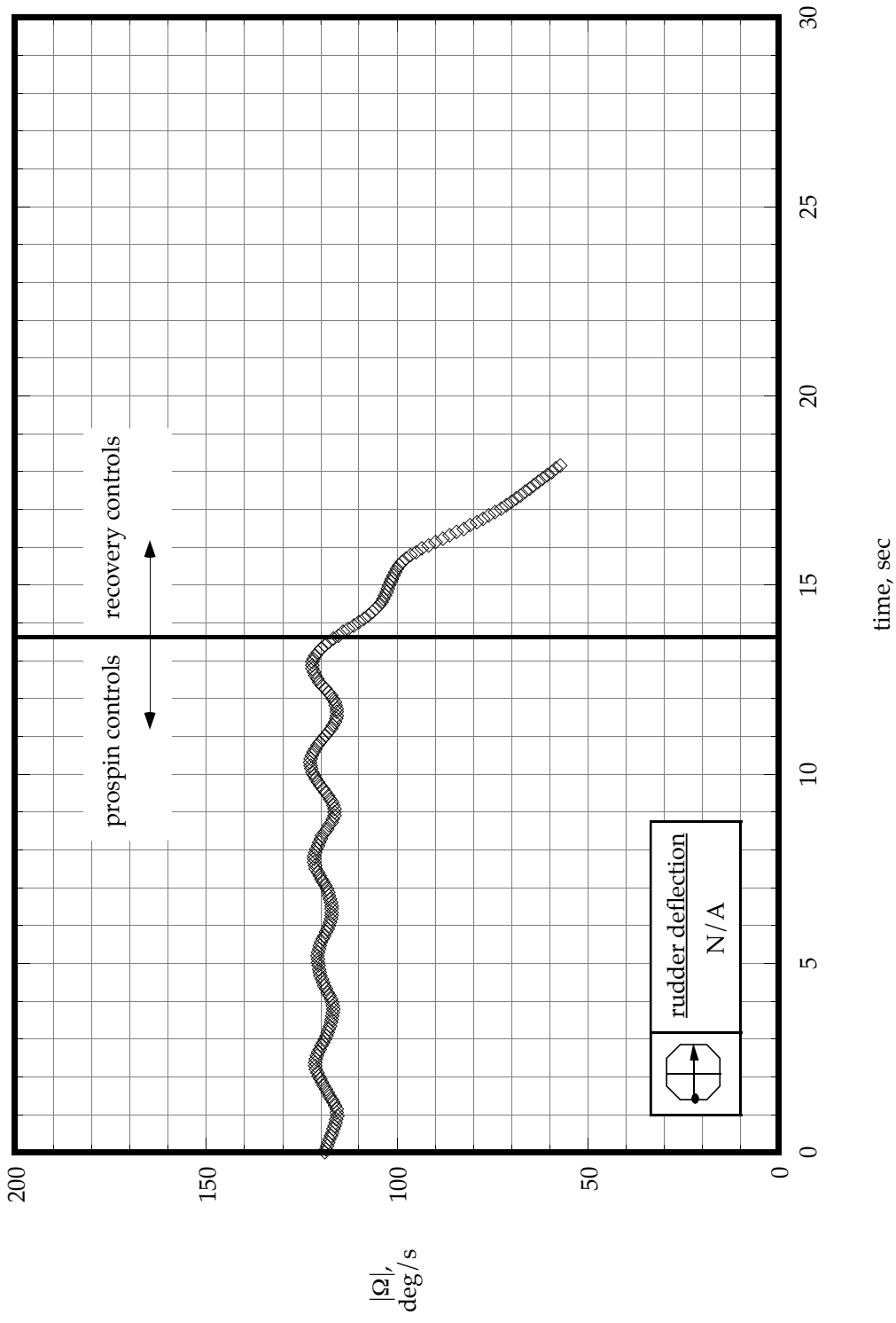
(b) vertical tails installed - rudders actuated (see test 5 - table 5).

Figure 9. Continued.



(c) vertical tails removed (see test 6 - table 5).

Figure 9. Continued.



(d) vertical tails removed - lateral controls with spin for recovery (see test 7 - table 5).

Figure 9. Concluded.

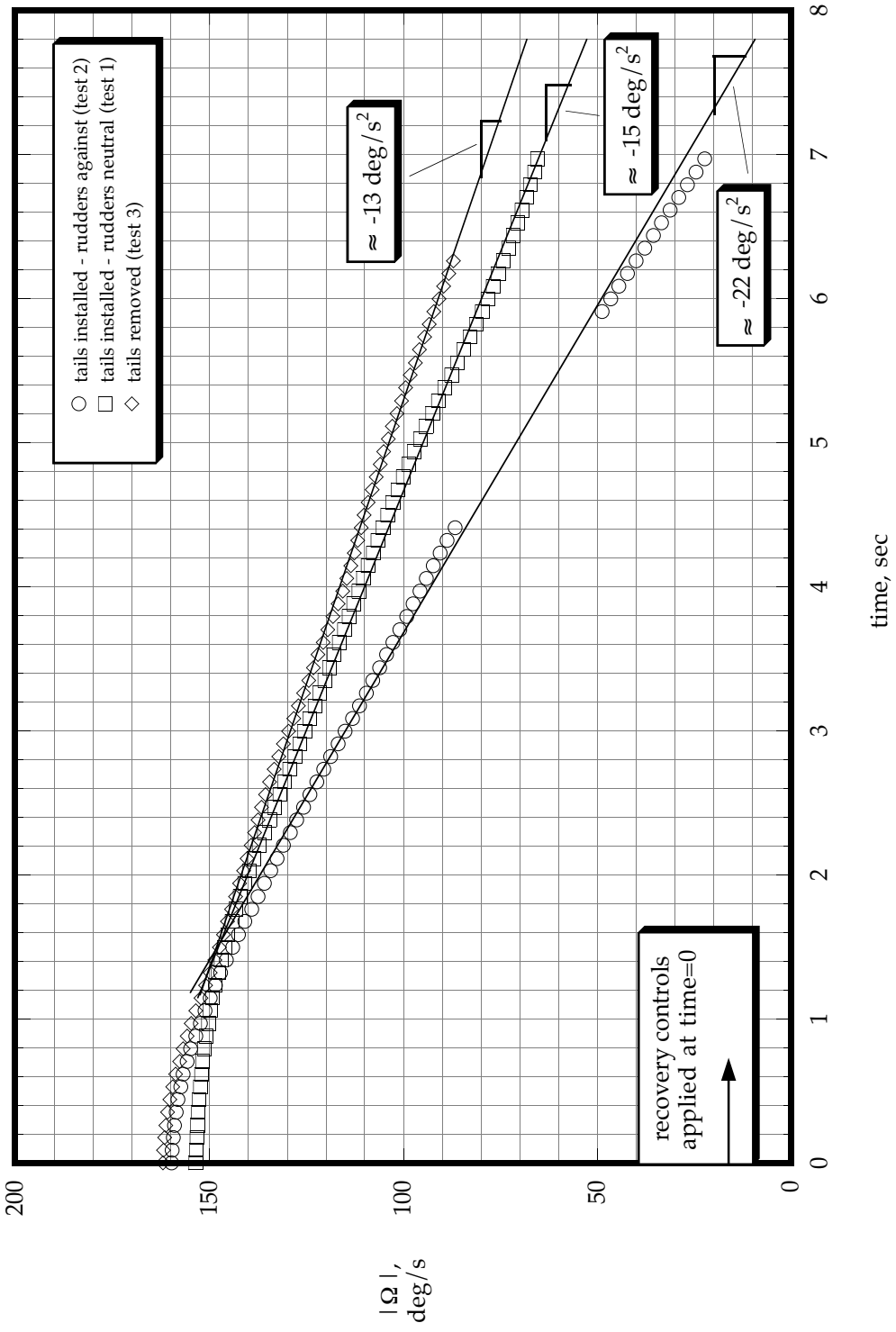
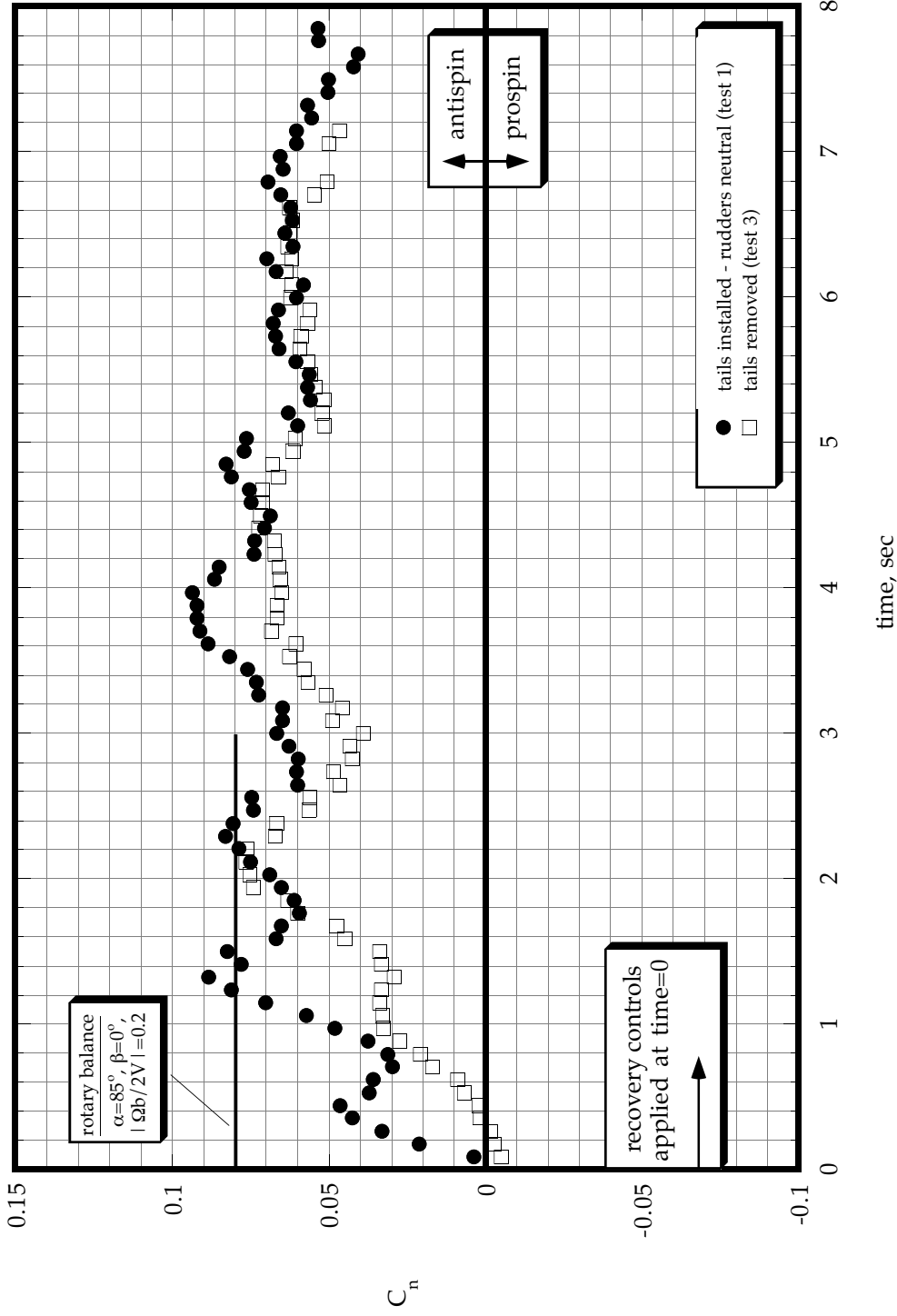
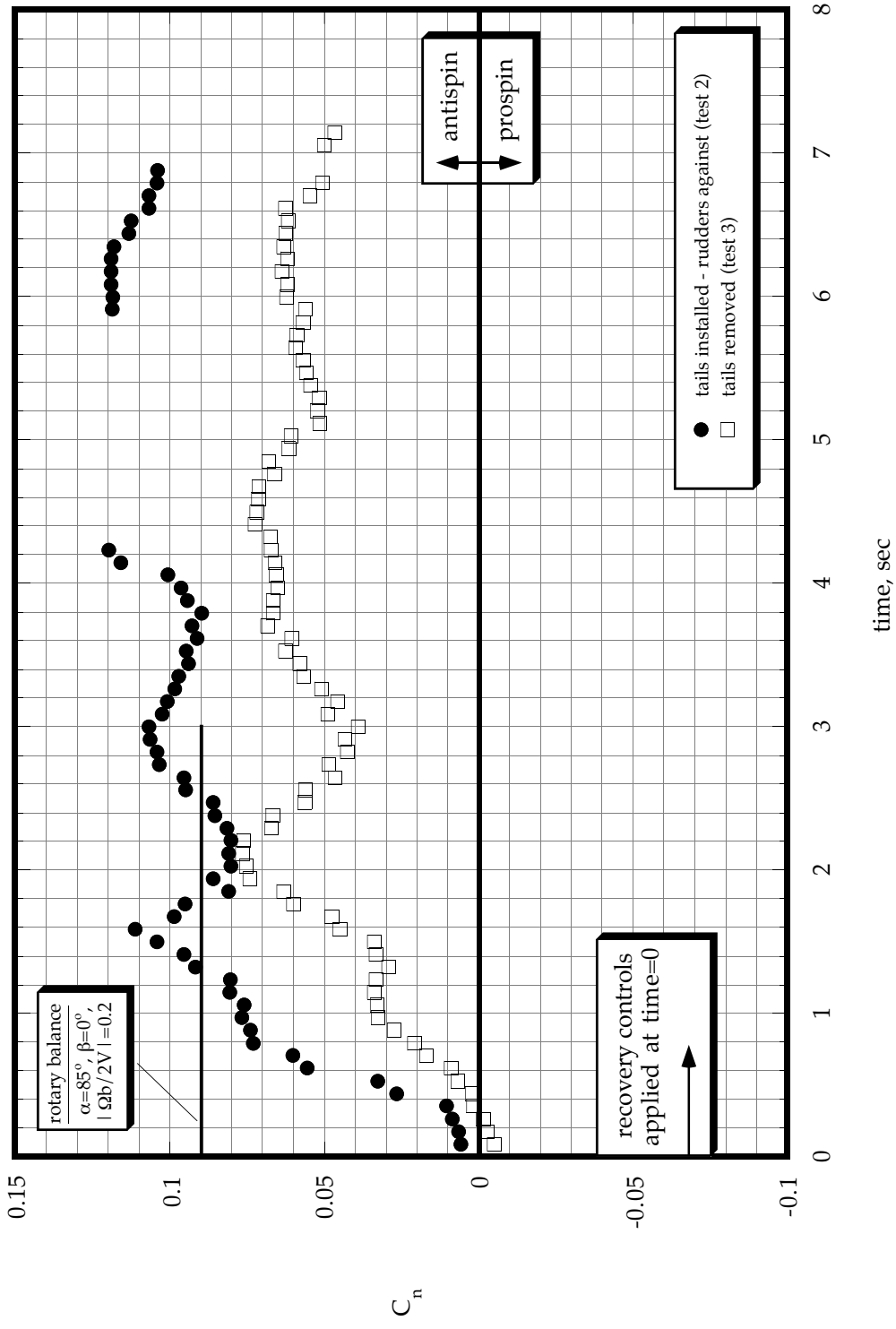


Figure 10. Angular deceleration during recovery from erect spins in table 4. Values shown are full-scale values converted from model-scale values.



(a) Vertical tails installed - rudders neutral (test 1) compared to vertical tails removed (test 3). Rotary balance data for same control surface deflections as those used in test 1.

Figure 11. Calculated aerodynamic yawing moment coefficient during recovery from erect spins in table 4. Values shown are full-scale values converted from model-scale values.



(b) Vertical tails installed - rudders against (test 2) compared to vertical tails removed (test 3).  
 Rotary balance data for same control surface deflections as those in test 2.

Figure 11. Concluded.